THE UNIVERSITY OF ALBERTA

BEHAVIOUR OF COMPOSITE BEAMS IN NEGATIVE BENDING

by

ELLYS BERT PIEPGRASS

A THESIS

SUBMITTED TO THE FACULTY OF GRADUATE STUDIES

IN PARTIAL FULFILMENT OF THE REQUIREMENTS FOR THE DEGREE OF

MASTER OF SCIENCE

DEPARTMENT OF CIVIL ENGINEERING

EDMONTON, ALBERTA

JUNE, 1968

THE UNIVERSITY OF ALBERTA

FACULTY OF GRADUATE STUDIES

The undersigned certify that they have read, and recommend to the Faculty of Graduate Studies for acceptance, a thesis entitled BEHAVIOUR OF COMPOSITE BEAMS IN NEGATIVE BENDING in partial fulfilment of the requirements for the degree of Master of Science.

ABSTRACT

This investigation forms a part of a continuing study of composite steel and concrete beams being conducted at the University of Alberta. The object of the overall program is to study the behaviour of continuous composite beams at all stages of loading up to the ultimate load and to propose criteria for design based on ultimate load considerations.

This thesis reports the results of tests on six simple span composite beams loaded to produce negative moment. The major variables considered were the amount of longitudinal reinforcement in the slab, and the width of the slab. It was found that the compression flange of some of the beams had to be stiffened to prevent premature failure by local buckling of the steel section.

As a result of these tests, it was concluded that the moment capacity of the composite section was increased by the addition of slab reinforcement, that the average stress in the reinforcement at ultimate load is less than the yield stress, and that the use of a compact steel section in a composite beam does not guarantee that sufficient rotation capacity will exist for the formation of a plastic hinge in the composite beam.

ACKNOWLEDGEMENTS

This investigation was made possible through financial assistance provided by the National Research Council of Canada.

The author wishes to extend his thanks and grateful acknowledgement to the following for their contributions toward the completion of the tests reported herein:

J. Longworth, Professor, Department of Civil Engineering, for his guidance, advice, and unstinting contributions of time during the preparation of this report.

Mr. H. Panse and staff of the Department of Civil Engineering, and others who assisted during the fabrication and testing of the beam specimens.

TABLE OF CONTENTS

LIST OF PLATES

LIST OF TABLES

LIST OF FIGURES

FIGURE		PAGE

CHAPTER I

INTRODUCTION

1.1 INTRODUCTORY REMARKS

The present investigation forms a part of a continuing study of continuous composite beams being carried out in the Department of Civil Engineering at the University of Alberta. The object of the study is to establish a theory for the behaviour of continuous composite beams over the full range of loading to failure and to propose design criteria based on ultimate load.

1.2 POSITIVE BENDING OF COMPOSITE BEAMS

The first phase of the study concerned the behaviour of composite beams in positive bending. A series of tests of simple beams was carried out by Ferrier in 1965[1]. The primary object was to measure experimentally and predict analytically the rotation capacity of simply supported composite beams subject to positive moment. The test program consisted of testing four beams representing two extremes in composite beam dimensions. Two of the beams had very heavy slabs which placed the neutral axis in the slabs. The remaining two had very light slabs in which the neutral axis was in the web of the steel beam section. The design of the shear connectors for these beams was based on the results of extensive research conducted at Lehigh University[8,9].

The behaviour of these beams was predicted analytically with good results. A computer program was then devised to incorporate the basic analysis together with the additional factor of strain hardening in the steel. Subsequently this computer program was modified by the author, replacing the linear stress-strain relationship for concrete previously used with a modified Hognestad stress block. FIGURE 1.1 shows the relationship between experimental results and the theoretical curves based on the various assumptions.

The analysis for all of the theoretical curves assumed complete interaction, and that failure by crushing of the concrete occurs when a limiting strain is reached at the extreme fibre of the concrete slab. Curves A and B are based on a linear stress strain relationship for the concrete, and a limiting concrete strain of 0.0038 inches per inch. Curve B is based on the same considerations as Curve A except that the strain hardening properties of the steel are included. Curve C assumes a limiting strain of 0.004 inches per inch in the concrete, strain hardening of the steel, and a Hognestad distribution of concrete stresses.

A further refinement in the analysis would be to consider the residual stresses in the steel beam section. Part of the difference between the experimentally obtained and the theoretical curves is undoubtedly due to the residual stresses in the steel. However, this factor would not affect either the moment or curvature at failure.

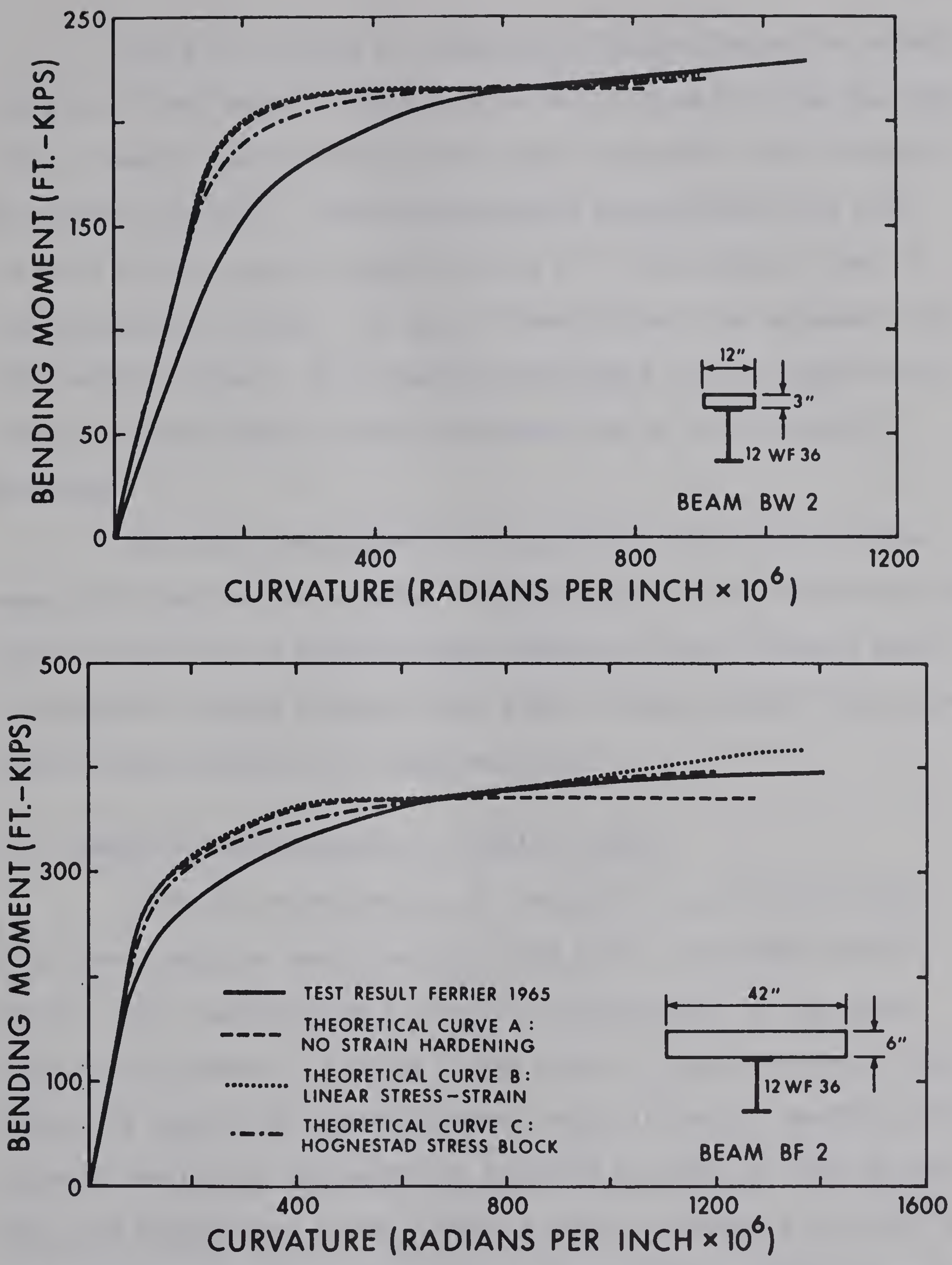

Figure 1.1 MOMENT CURVATURE RELATIONSHIPS FOR POSITIVE BENDING

Curve A of FIGURE 1.1 consistently underestimates the moment capacity of the composite section at failure. Curve B in one case predicts a moment capacity which is too high, but predicts the curvature at failure very well. Curve C consistently underestimates the curvature at failure, but the shape of Curve C is the closest to that of the experimental curves. For each of these curves, the agreement with test results is good. It is therefore concluded that the behaviour of composite beams subject to positive moment can be satisfactorily predicted.

The design requirements for composite beams under positive moment are contained in Canadian Standards Association Standard S16-1965 and in Association of American State Highway Officials Standard Specifications for Highway Bridges 1965. Both of these consider only conventional elastic analysis for composite beams.

1.3 COMPOSITE BEAMS SUBJECTED TO NEGATIVE MOMENT

With the increasing use of continuity in structural design, continuous composite beams have also been built. The AASHO Specifications allow consideration of the slab reinforcement in the computation of the moment of inertia in the region of negative moment. No mention is made of the negative moment region in the CSA Specifications. Standard practice in the design of buildings has been to count on only the steel beam section in the region of negative moment, and to utilize the full composite section at midspan. To control the width of cracks in the regions of negative moment, appreciable amounts of slab rein-

forcement are often added. It is conceivable that appreciable economy could be achieved if the reinforcement introduced to control cracking could be considered in the determination of the moment capacity of the composite section, and if design of continuous beams could be based on plastic design concepts. If this is to be done, however, more knowledge of the behaviour under negative moment must be obtained in order to establish a rational design procedure.

In a structural steel flexural member, care must be taken to prevent premature buckling of the thin steel compression elements. In a composite beam subjected to positive moment the concrete slab, the compression element of the composite beam, is not likely to buckle. Furthermore, through natural bond and by means of mechanical shear connectors, the slab restrains the top flange of the steel section from buckling, should it be under a compression stress. As far as the effective concrete flange width contributing to the action of a composite beam is concerned, the situation is similar to a reinforced concrete tee beam, and design provisions governing effective flange widths of these two types of beams are identical.

The situation is considerably different in the region of negative moment. In this case, the tension flange, not the compression flange, of the steel beam section is in contact with the concrete slab. Therefore, the buckling tendencies of the compression flange are more critical than in a positive moment region. The slab will crack under relatively light loads. Because of this cracking, the effective slab width may differ from that in the region of positive

bending. There is also the possibility that the cracking of the slab may affect the mechanism of shear transfer between the slab and beam.

Among the various aspects of flexural behaviour of a composite section in a region of negative moment, three are of major significance. The effectiveness of longitudinal slab reinforcement in increasing the moment capacity of the section must be established. The nature and extent of cracking of the slab and the effect of cracking on the effective flange width should be examined. It must also be established whether hinging occurs, and if sufficient rotation capacity can be developed so that redistribution of moments can be realized. In addition to these aspects, information is necessary concerning shear connection, anchorage requirements, contribution of transverse reinforcement, and the possible types of secondary failures.

None of these aspects has been completely examined in the present investigation. However, certain significant information has been obtained, and recommendations for further research can be made.

CHAPTER II

REVIEW OF RESEARCH

2.1 INTRODUCTION

As previously noted, the behaviour of composite beams under positive moment has been quite thoroughly investigated. Much less investigation has been done on negative moment bending. As far as can be ascertained, the present investigation represents the first attempt to test composite beams under negative moment only. Though other investigators have not isolated the negative moment region, several have studied the behaviour of continuous composite beams.

2.2 SIESS AND VIEST

In 1953 Siess and Viest[2] tested two 1/4 scale composite bridge decks. The beams of one bridge contained shear connectors over the entire length; in the other shear connectors were omitted in the negative moment regions. Longitudinal slab reinforcement was .99% of slab area or approximately 16% of the steel beam section area. It was concluded that the slab reinforcement can act compositely with the beam in the negative moment region, but the concrete of the slab makes no contribution. The interaction between the steel beam section and the slab reinforcement was described as "practically complete" for the bridge with shear connectors, and

"about half way between complete and no interaction" for the bridge without shear connectors. Ultimate failure of the bridge was due to punching shear failure of the slabs before the ultimate flexural capacity of the composite beams was reached. No lateral or local buckling of the steel sections occurred.

2.3 CULVER, ZARZECZNY, AND DRISCOLL

In 1961 Culver, Zarzeczny, and Driscoll[3] tested one continuous composite beam to investigate the feasibility of the use of plastic analysis and ultimate strength theory. This beam was reinforced with temperature steel only in the longitudinal direction. One very large crack formed in the slab over the center support, and the ultimate load was reached when the slab at this point began to twist. The authors observed that plastic design loads were reached. No buckling of the steel section was noted. It was concluded that the plastic moment capacity of the steel section could be used in design, and they recommended an expansion joint to control cracking. No contribution of the longitudinal temperature steel to the moment was considered.

2.4 SLUTTER AND DRISCOLL

In 1962 Slutter and Driscoll[4] proposed a design for continuous beams based on the concepts of simple plastic theory. They recommended a negative moment capacity equivalent to the plastic moment based on complete yielding or plastification of the

steel in the cross section including longitudinal reinforcing steel provided shear connectors are present in the region of negative moment.

2.5 BARNARD

In 1963 Barnard[5] tested a series of four continuous three-span composite beams. Flexible shear connectors were provided throughout the beam length. Longitudinal reinforcement was either 2.5% or 0.89% of slab area, being approximately 47% or 17% of the steel beam section area. Two beams failed by concrete crushing in the positive moment regions and two failed by formation of an S-shaped buckle of the steel beam in the negative moment region (accompanied by a shear failure of the slab in one case). Considerable slip and loss of interaction was noted, but moment-curvature relationships observed were still in good agreement with computed values. The width/thickness ratios for the outstanding flange and for the web of the steel section were approximately 5.4 and 20.6 respectively.

2.6 DANIELS AND FISHER

In 1966 Daniels and Fisher[6,7] tested a series of four two-span continuous composite beams, first under dynamic loading, and then under static load to failure. In the negative moment region, the slab reinforcement, as percentage of slab area, was 0.61%, 0.61%, 1.96%, 4.50%, and as percentage of steel section area was approximately 12%, 12%, 38%, and 88%. All beams developed

local flange and web buckles. For the two lightly reinforced beams which had only one full depth and two half depth bearing stiffeners at the center support, the maximum negative moment was significantly less than that predicted, and with further load, the moment decreased sharply. For the two most heavily reinforced beams which had a total of five full-depth and two half-depth stiffeners at the center support, negative moment sections achieved moments closer to that predicted, and these moments were maintained through a considerable rotation. Three of the beams exceeded the predicted ultimate load and the other carried 97% of the predicted value. Daniels and Fisher concluded that redistribution of moments had occurred, and that the lower moment capacity in the region of negative moment had been compensated by a higher than predicted moment capacity in the positive moment region. The width/thickness ratio for the outstanding flanges of the steel section varied from 13.85 to 14.75, and the width/thickness ratio for the webs varied from 47.80 to 49.00

2.7 SUMMARY

In brief, previous investigations have shown that in a negative moment region of a composite beam, longitudinal slab reinforcement contributes to the moment capacity of the composite section. However, it has not established whether or not there is an upper limit to this increase in capacity. Also, it appears that the interaction between the longitudinal slab reinforcement and the steel beam section is not complete. Furthermore, buckling of the compression flange of the steel beam is possible.

CHAPTER III

TEST PROGRAM

3.1 SCOPE OF INVESTIGATION

This present investigation is a study of behaviour of a composite beam section in an isolated negative moment region. It involves two major variables. The first is the effect of the longitudinal slab reinforcement on the moment capacity of the composite section. The second is the effect of slab width on the behaviour of the beam. It was not originally intended to vary the width/thickness ratio of the steel beam section, but it was found necessary to modify the test beams in order to fully explore the effect of the longitudinal slab reinforcement.

3.2 DESIGN OF TEST SPECIMENS

3.2.1 CHOICE OF STEEL SECTION AND BASIC BEAM DIMENSIONS

In order to facilitate the casting, handling, and testing of the beam specimens, it was decided to use a fairly light slab and a light steel section. A 3-inch slab thickness and a 12B16.5 steel section were therefore selected. The span length chosen was 8'-0". This length of negative moment region was considered compatible with a span length of about 20 feet which might be expected in a practical situation for a continuous

span. The test specimens were made 10'-0" long, thus providing anchorage for the longitudinal reinforcement beyond the support.

This combination of slab and steel beam section is listed as an economical section in the Bethlehem steel manual[10] for elastic design for composite beams in positive bending. The 12B16.5 section, when rolled of G40.12 steel is considered a compact section according to CSA Standard S16, but the width/thickness ratios of 14.9 for the flange and 46.8 for the web of the steel section are very close to the code limit.

3.2.2 LONGITUDINAL SLAB REINFORCEMENT AND FLANGE WIDTH

In order to study the two major variables, two series of beams were designed. The four beams of the first series were intended to be identical except for amounts of slab reinforcement and numbers of shear connectors. However, it was found necessary to modify BEAMS 1 and 2 in order to develop the strength of the reinforcement provided. The three beams of the second series were identical except for the width of the slab and the spacing of the reinforcing bars. BEAM 2 is considered part of series one and also part of series two.

Concrete slab widths varied from 3'-0" (for all beams of the first series) to 5"-0". For positive moment CSA Standard S16 allows a maximum effective flange width of 2'-0" for an 8'-0" span length and a maximum of 4'-4" for a three-inch slab thickness for spans greater than 17'-4" in length. The 3'-0" width was justified

on the assumption that the negative moment region was only part of a longer span. The 5'-0" width was chosen in order to provide a fairly wide range over which to study behavioural differences. The two series also presented an opportunity to analyse the cracking behaviour of composite beams in relation to amount of reinforcing steel provided.

3.2.3 DESIGN TO PREVENT SECONDARY FAILURES

Previous investigations indicated the possibility of secondary failures due to inadequate shear connection, longitudinal cracking along the beam centerline, insufficient anchorage of slab reinforcement and buckling of the steel beam section. The test specimens were designed to prevent failure by the first three of these mechanisms.

1/2-inch by 2-inch headed shear connectors were employed in all test specimens. Culver, Zarzeczny and Driscoll[3] recommended an ultimate shear of 14.0 kips for this size of connector. CSA Standard S16 permits an allowable shear of 5.1 to 5.9 kips per connector depending on concrete strength. Five of the test beams were designed on the basis of an ultimate capacity of 10 kips per connector. BEAM 3 was designed on the basis of 14 kips per connector. The total number of connectors was computed on the basis that the shear to be resisted in each half span equalled the force required to produce yielding of the slab reinforcement. The connectors were spaced uniformly along the span.

Transverse reinforcement was provided to control longitudinal cracking. In Barnard's[5] tests, longitudinal cracking occurred when only wire mesh was provided, but did not occur when the ultimate moment sections were reinforced with additional transverse reinforcement in the amount of 0.56% of slab area. The area of steel provided by the wire mesh is not known. One series of beams tested by Culver, Zarzeczny and Driscoll[3] at Lehigh University contained transverse reinforcement in the amount of 1.29% of slab area. No longitudinal cracking was reported. Ferrier[1] encountered longitudinal cracking of the slab with transverse steel of 0.20% of slab area. The beams in this present investigation were reinforced with #3 transverse bars at 6-inch spacing over the entire length, giving a ratio of transverse reinforcement to slab area of 0.61%.

Protection against anchorage failure was provided by continuing the longitudinal bars into the 1'-0" length of slab which existed beyond the support at each end of the beam.

The test specimens were not designed to preclude the possibility of failure by buckling of the steel section. However, stiffeners were provided at the centerline and at the support points (1'-0" from each end). These stiffeners were 3/8" plate welded to the web and both flanges of the beam by continuous welds. It became apparent when the two beams with the least longitudinal slab reinforcement failed by buckling of the steel

section that, in order to investigate the full effects of the longitudinal reinforcement, the compression flanges of the steel sections had to be stiffened. Accordingly, the compression flanges of the remaining beams were coverplated with 3" x 3/8" plate. The width/thickness ratio for the flange with coverplate was approximately 6.0.

A summary of the details of the test specimens is presented in FIGURES 3.1 and 3.2.

3.3 FABRICATION OF TEST SPECIMENS

All steel beams sections were fabricated from G40.12 material of the same heat lot by Canada Iron Foundries Ltd. of Edmonton. Fabrication included installation of bearing stiffeners and headed stud shear connectors. The fabricator also supplied a length of the same 12B16.5 material for material tests, and subsequently supplied five 3" x 3/8" strips of A36 material which were used as coverplates.

The coverplates were welded to the compression flange of the test specimens by University Technical Services. On the first beam to which a coverplate was added, welding produced a deflection of approximately 1/4" after cooling. The process was refined until no warping was noted on the final beams coverplated.

PLATE 3.1(a) shows the steel beam section in place prior to the casting of the concrete slab. The forms consisted of two low platforms with side boards which could be fastened into any

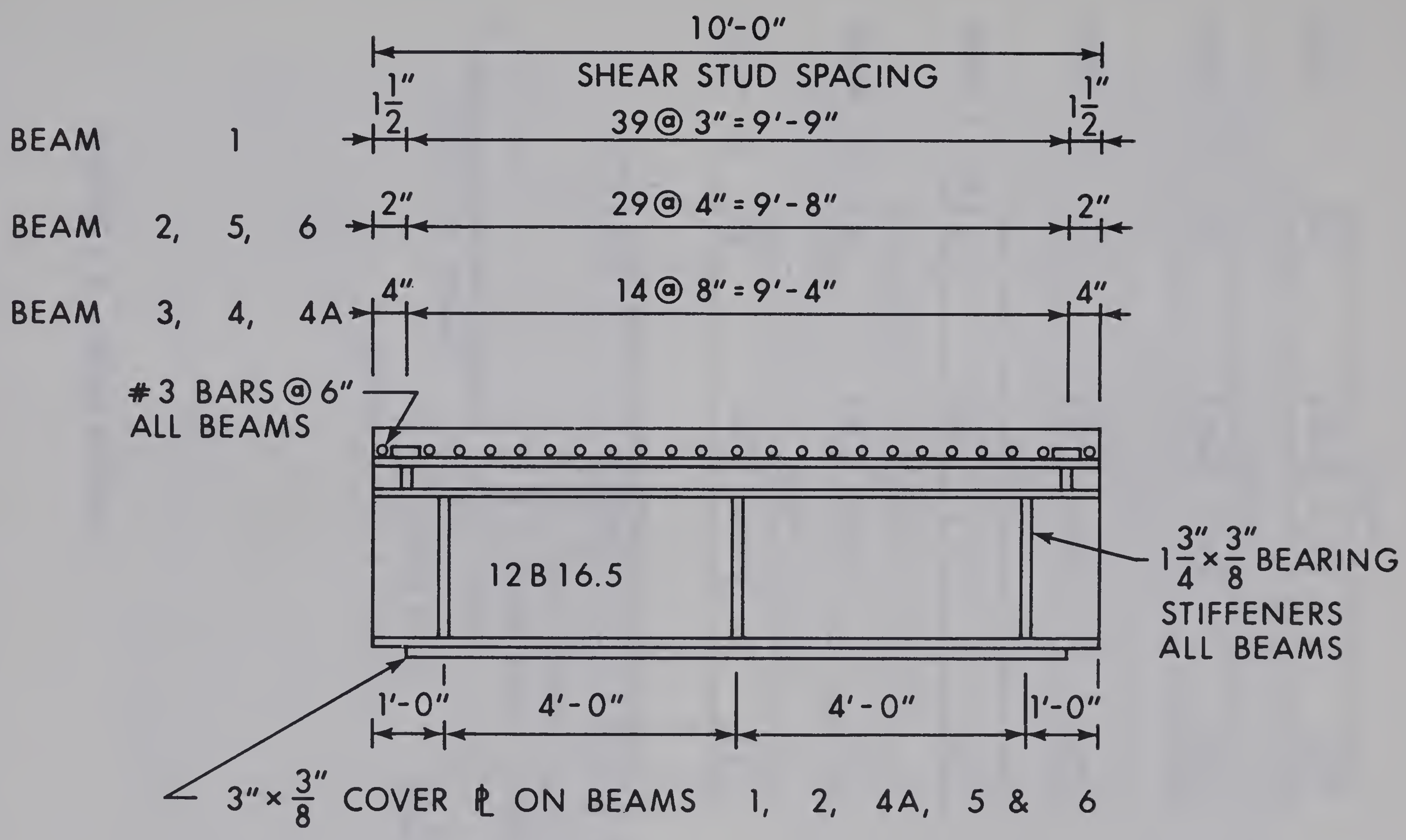

FIGURE 3.1 BEAM DETAILS

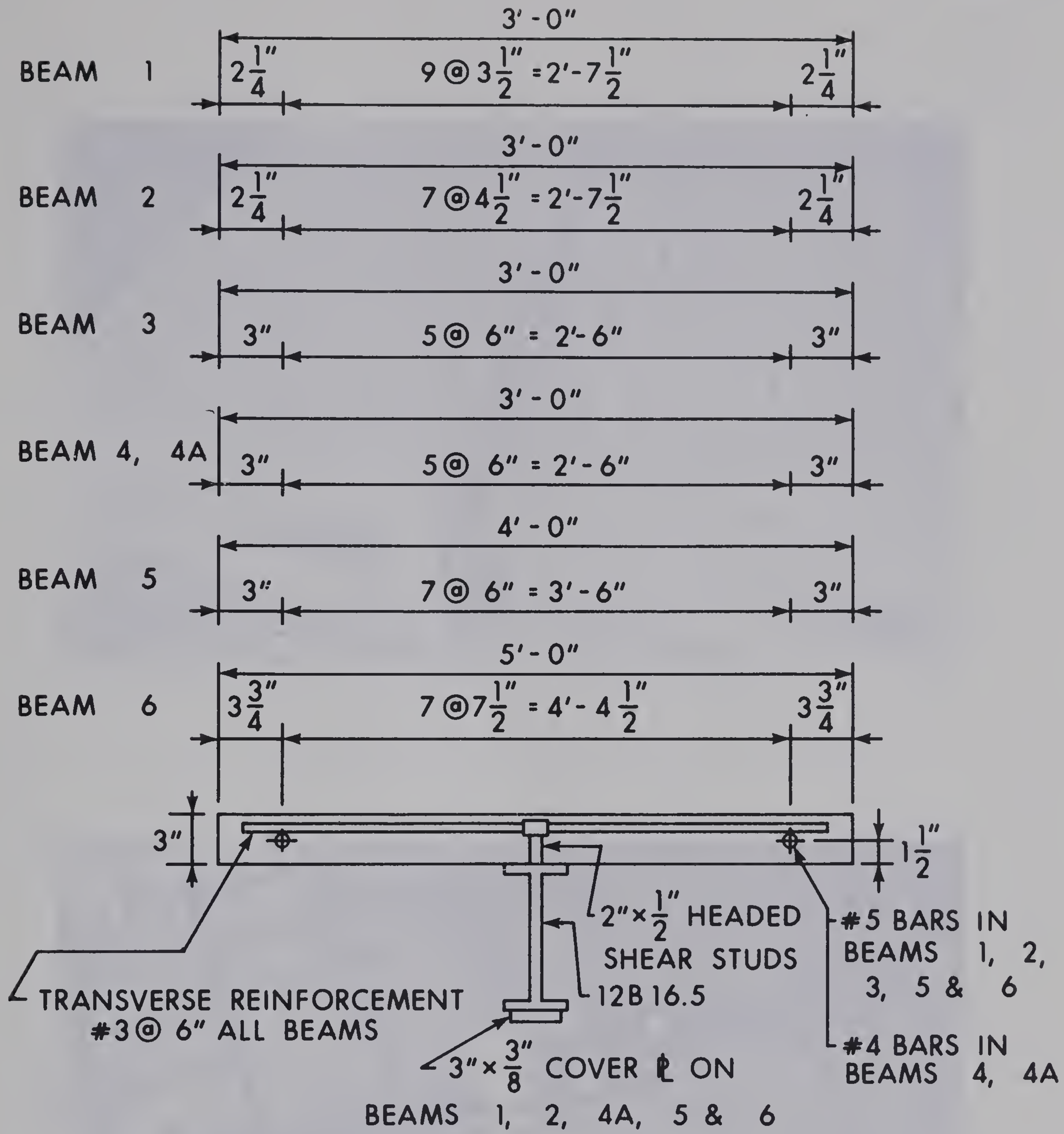

FIGURE 3.2 BEAM DETAILS

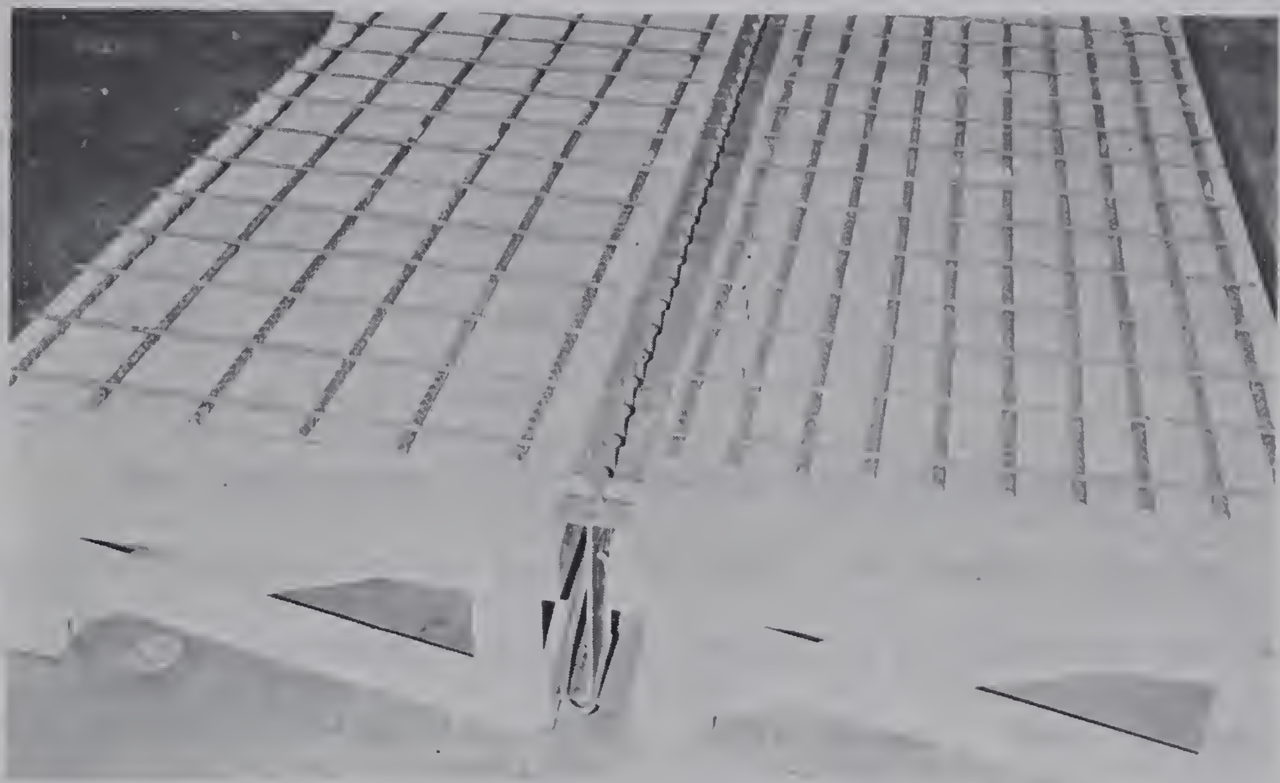

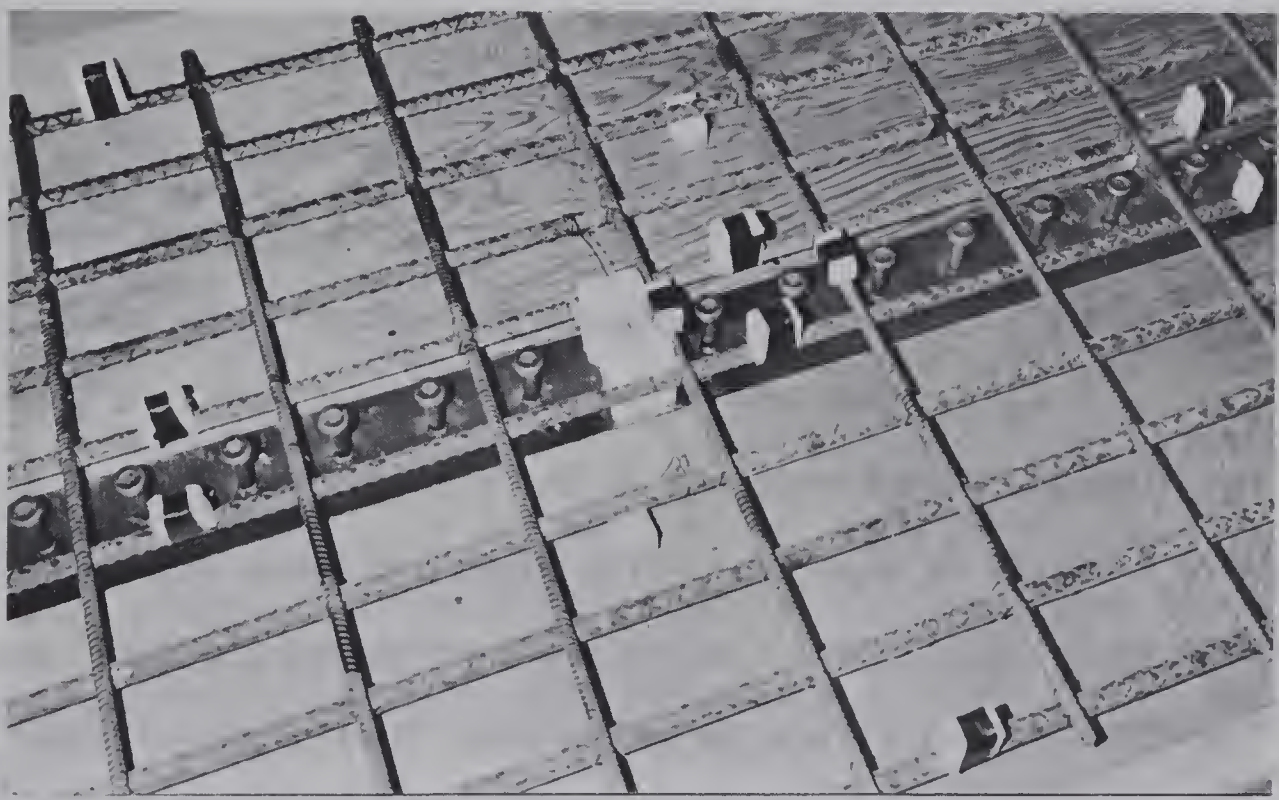

PLATE 3.1 VIEWS PRIOR TO CASTING

position by long wood screws. The steel beam section was suspended by the flange tips into position between the two platforms. The forms were then fastened in the proper position by the side boards, and the steel section was adjusted into a vertical position by means of wedges. The forms were 32 feet long, allowing the simultaneous casting of three beams.

The longitudinal and transverse slab reinforcement was prepared by first tying the bars into mats. At twenty selected points, the reinforcement was sanded smooth in preparation for the attachment of electrical resistance strain gauges. Small blocks of Styrofoam were taped to these locations to form voids in the concrete which were necessary for the application of electrical gauges after the concrete was cast and cured. Similar treatment was applied to two locations on the tension flange.

The reinforcing mats were positioned in the forms on small wooden blocks dimensioned so as to locate the centroid of the longitudinal reinforcement at mid-depth of the slab. PLATE 3.1(b) shows the mat just prior to casting of the slab.

The concrete was mixed in the Structural Laboratory's nine cubic foot mizer and every effort was made to obtain a uniform product. The mix proportions are noted in TABLE 3.2. Each of the four beams having a 3'-0" slab width was cast from one batch of concrete. BEAMS 5 and 6 were cast from three batches; one placed at the midspan section of each beam, and the third to complete the two slabs. The 3-inch slump concrete was mechanically vibrated.

The concrete was moist cured for three days, after which the Styrofoam was chipped out and the strain gauges installed.

3.4 MATERIAL PROPERTIES

The concrete and steel properties are summarized in TABLES 3.1 and 3.2. Six concrete cylinders were cast with each beam, and two additional cylinders were cast from the seventh batch of concrete. Both the beams and cylinders were moist cured for three days, then stored in laboratory conditions. Two cylinders from each batch were tested at seven days, and the remainder were tested on the day of the beam test. Half of the cylinders were tested in compression, and half were subjected to a splitting tensile test.

It will be noted from TABLE 3.1 that tension strength decreased with age for batches 1 and 2. The mix design was such that excessive shrinkage occurred, and this is probably the reason for this decrease. Compression strengths were higher than intended. However, it was decided to use the same mix for all beams rather than adjust it and introduce another variable.

Tension tests were performed on the reinforcing steel and structural steel used in the tests, and the results are presented in TABLE 3.2. An 18-inch section of 12B16.5 was cut into coupons, two from each flange and three from the web. Coupons were also taken from each coverplate.

BATCH No.	BEAM	AGE AT TEST (days)	COMPRESSION STRESS (psi)	SPLITTING TENSION (psi)
1	1	7 62 62	4,400 4,860 5,160	432 413 363
2	2	7 52 52	4,630 5,160 5,390	500 487 465
3	3	7 33 33	4.230 4,790 5,050	430 416 484
4	4	7 22 22	4,720 5,310 5,170	446 482 526
5	5	7 36 36	4,550 5,170 5,140	413 474 452
6	6	7 38 38	4,250 4,640 4,320	442 552 511
7	5 & 6	7	4,610	446

MIX PROPORTIONS:

CEMENT (HIGH EARLY)	185 lbs.
WATER	100 - 109 lbs.
SAND	483 lbs.
GRAVEL (3/4-inch)	504 lbs.
YIELD	8.5 cu. ft.

TABLE 3.1 CONCRETE DATA

SLAB REINFORCEMENT			STEEL BEAM SECTION			
TYPE	P_y (lbs)	σ_y (ksi)	TYPE	σ_y (ksi)	ε_{SH} (in./in.)	E_{SH} (psi x 10^6)
#3 BARS	5,870	53.4	WEB STEEL	47.3	.0094	.705
	5,780	52.5		49.3	.0063	.572
	5,900	53.6		49.0	.0056	.572
#4 BARS	9,600	48.0	FLANGE STEEL	43.7	.0064	.432
	9,450	47.2		44.6	.0096	.352
	9,450	47.2		44.4	.0132	.406
	9,600	48.0		43.6	.0135	.726
	9,600	48.0				
#5 BARS	14,550	46.9	COVER PLATE			
	14,450	46.6	1	47.2	.0212	.665
	14,600	47.1	2	47.5	.0189	.160
	14,850	47.9	4A	47.5	--	-
	14,650	47.2	5	46.2	.0208	.665
	15,200	49.0	6	46.3	.0200	.561

P_y - YIELD LOAD

σ_y - STRESS AT YIELD

ε_{SH} - STRAIN AT INITIATION OF STRAIN HARDENING

E_{SH} - INITIAL STRAIN HARDENING MODULUS

TABLE 3.2 STEEL PROPERTIES

3.5 INSTRUMENTATION

Because of the exploratory nature of this investigation, instrumentation varied somewhat from beam to beam. Four types of measurements were taken. Strains in the slab reinforcement and the steel beam were measured by means of SR4 type A7 electrical resistance strain gauges. Some strains were also measured by means of a Demec mechanical strain gauge of 8" gauge length. Deflections were measured by Mercer dial gauges and end rotations were measured by means of rotation gauges.

A7 strain gauges were positioned at twenty locations on slab reinforcement. Four locations were on the transverse bars, and 16 were on longitudinal bars as shown on FIGURE 3.3. On BEAMS 1 to 4, all twenty gauges were installed. Eleven gauges were installed on BEAMS 5 and 6. The positioning of strain gauges and Demec points on the steel beam section is illustrated in FIGURE 3.4. On BEAM 2, six additional gauges were installed to form a second gauge line on the beam web 15" from the centerline of the span. On beams which were not coverplated, only two gauges were placed on the compression flange. On BEAM 3, the first beam tested, strain gauges were positioned on the flange tips of each steel section and two sets were placed at mid-depth along the edge of the slab.

Four dial gauges were used to measure centerline deflections. Two gauges rested on the concrete slab about one inch from

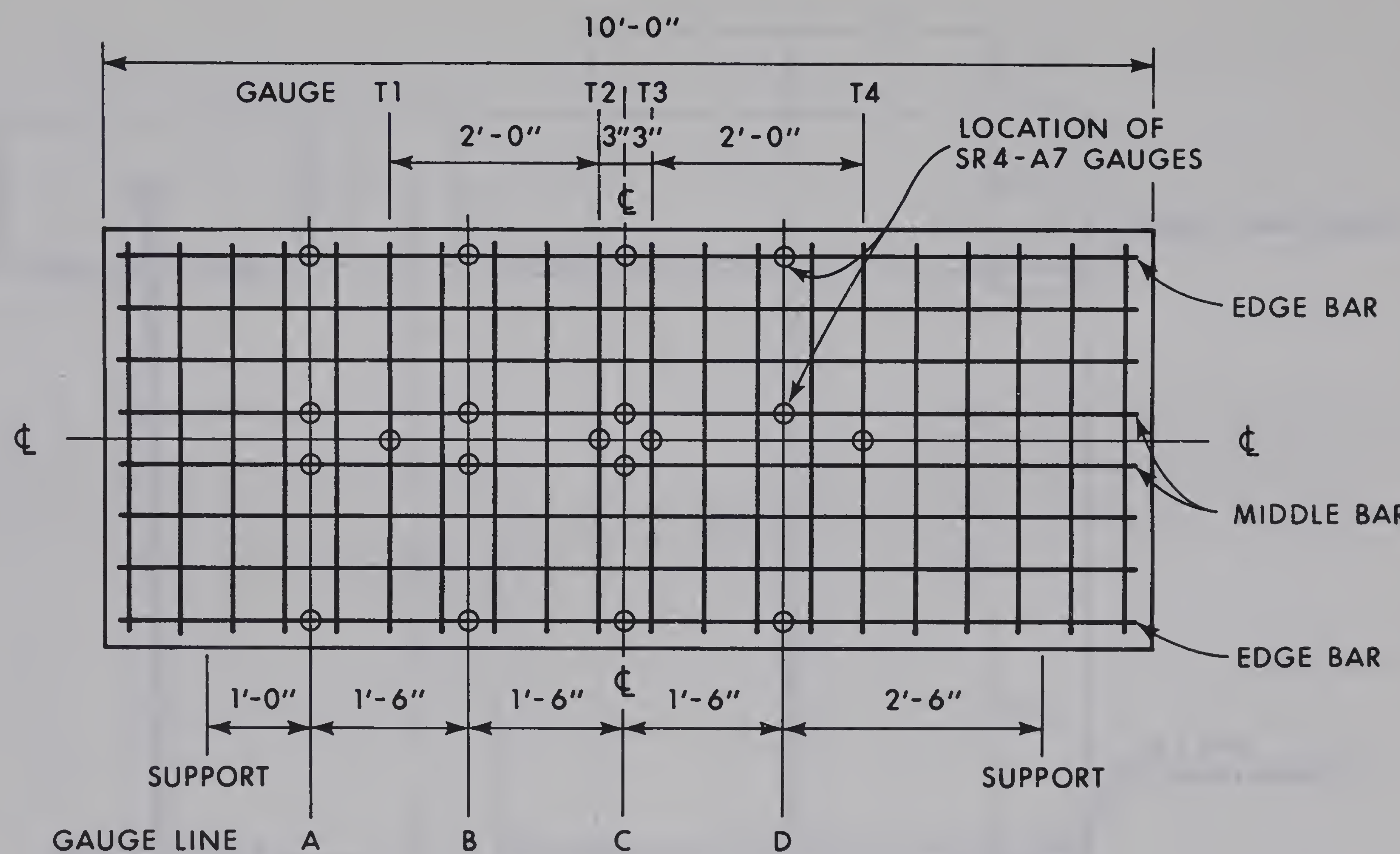

FIGURE 3.3 GAUGE LOCATIONS FOR SLAB REINFORCEMENT

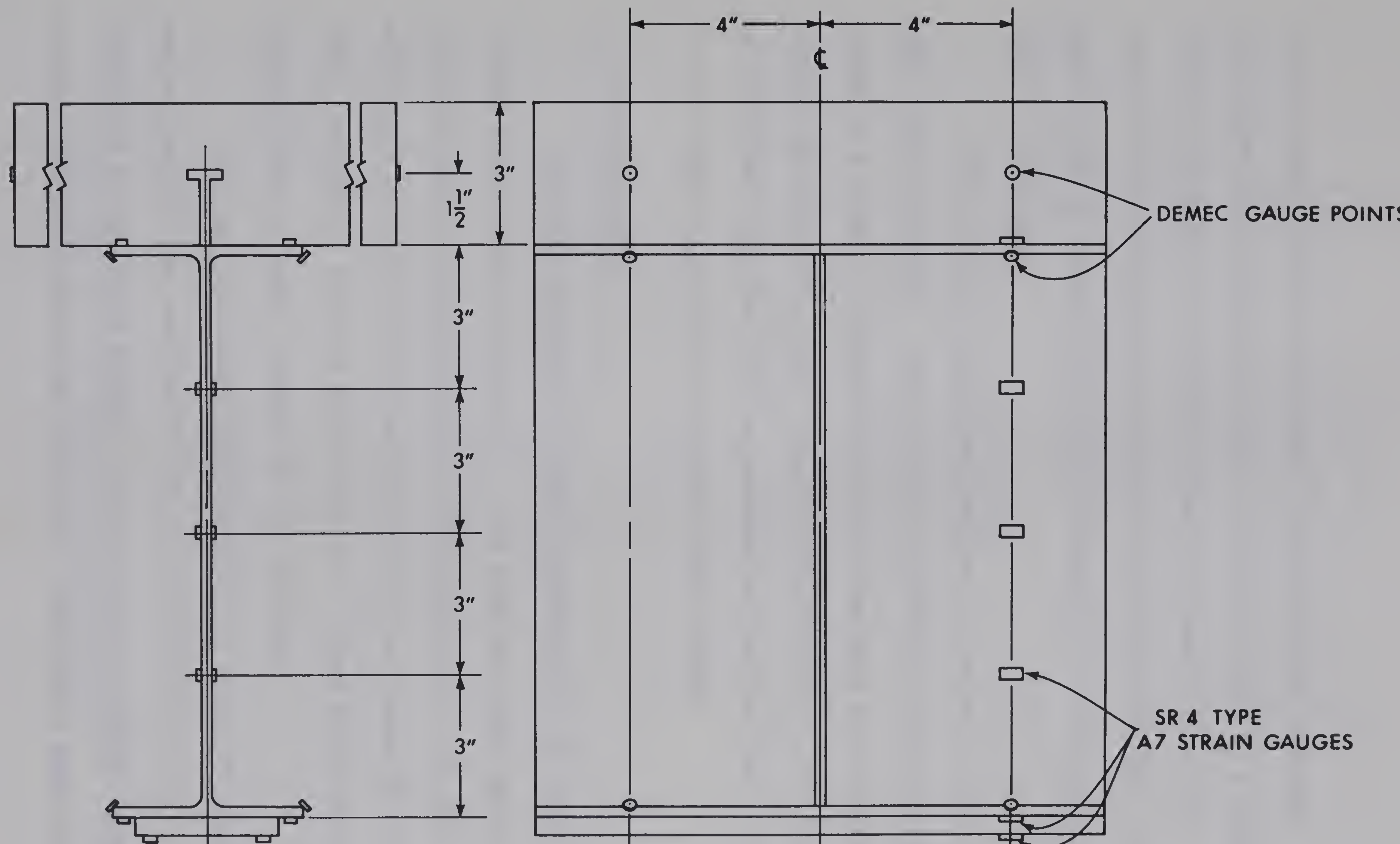

FIGURE 3.4 INSTRUMENTATION OF STEEL BEAM SECTION

the slab edges and two were placed adjacent to the beam web. The dial gauges were mounted by means of magnetic bases on a supporting channel attached to the loading frame. On some of the test specimens two additional dial gauges were mounted on one transverse support beam to measure any relative movement of the slab with respect to the support.

The rotation gauges were bolted to the web of the steel beam, one at each end. These gauges consisted of two arms connected by a hinge. One arm rotated with the beam and the other was levelled by means of a level tube and extention dial. Rotations were obtained from the relative movement of the two arms in a 15-inch length measured to the nearest 0.001 inches.

3.6 TEST EQUIPMENT

The test equipment is shown schematically on FIGURE 3.5, and can also be seen on PLATE 3.2. The beam specimens were tested with the slab on the underside and load applied by a 110 kip Amsler jack bearing directly on the compression flange of the steel beam at midspan. The jack reacted against a beam which was supported by four columns anchored to the load bed.

The test specimens were supported by transverse beams bearing against the concrete for the full width of the slab. Plaster of Paris placed between the slab and the support beams ensured that good bearing was obtained. One support beam rested

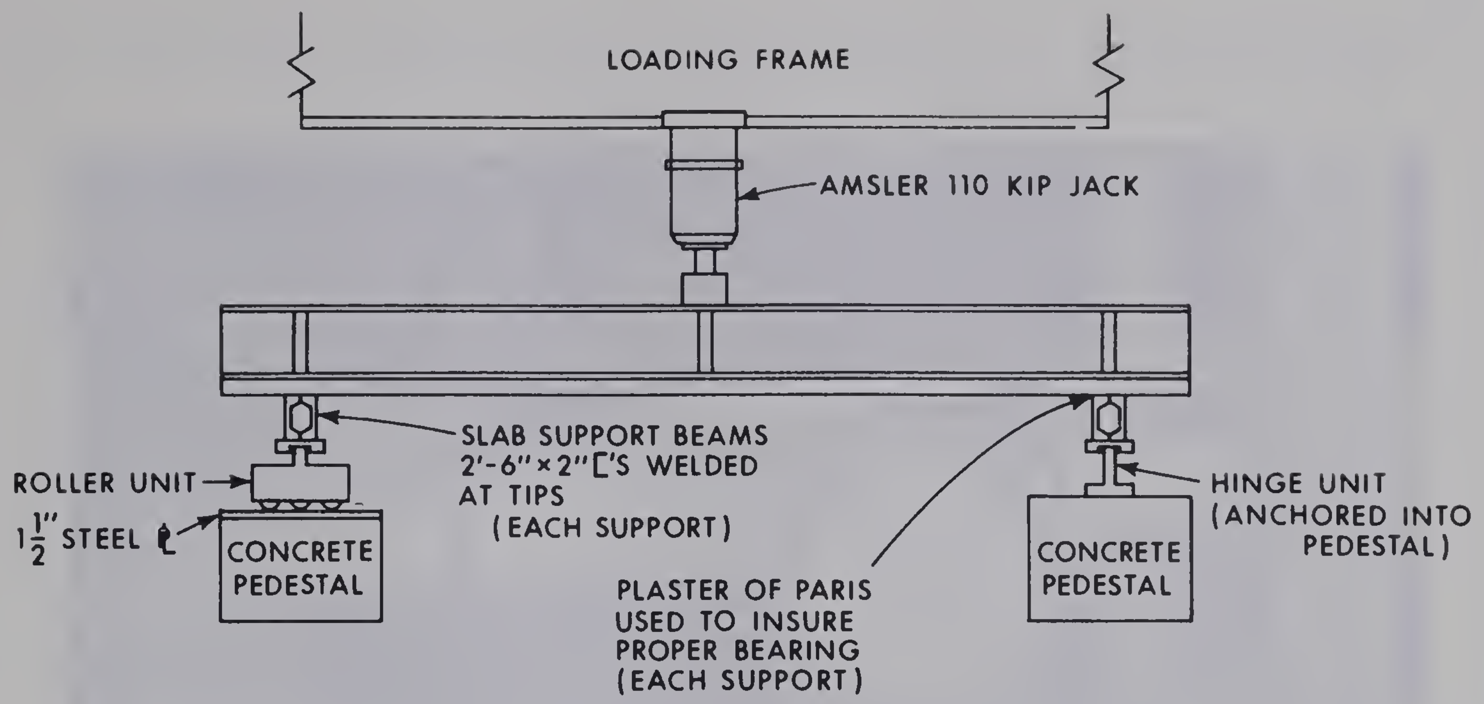

(a) LONGITUDINAL VIEW

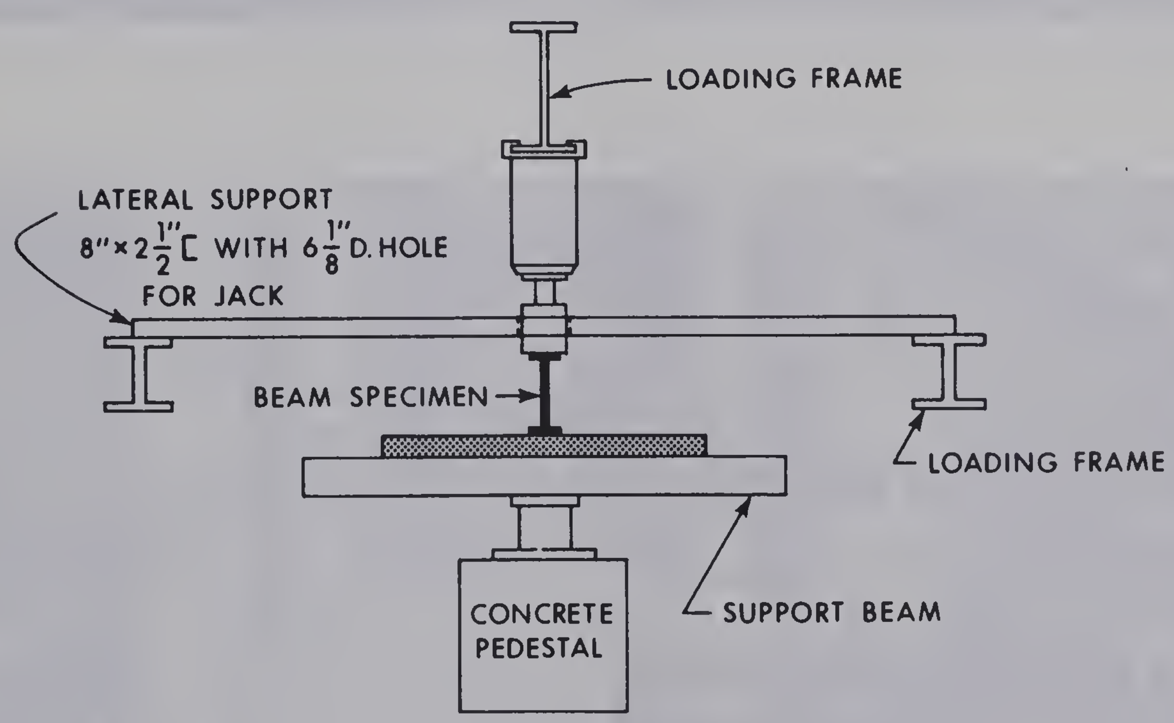

(b) TRANSVERSE VIEW

FIGURE 3.5 TESTING ARRANGEMENT

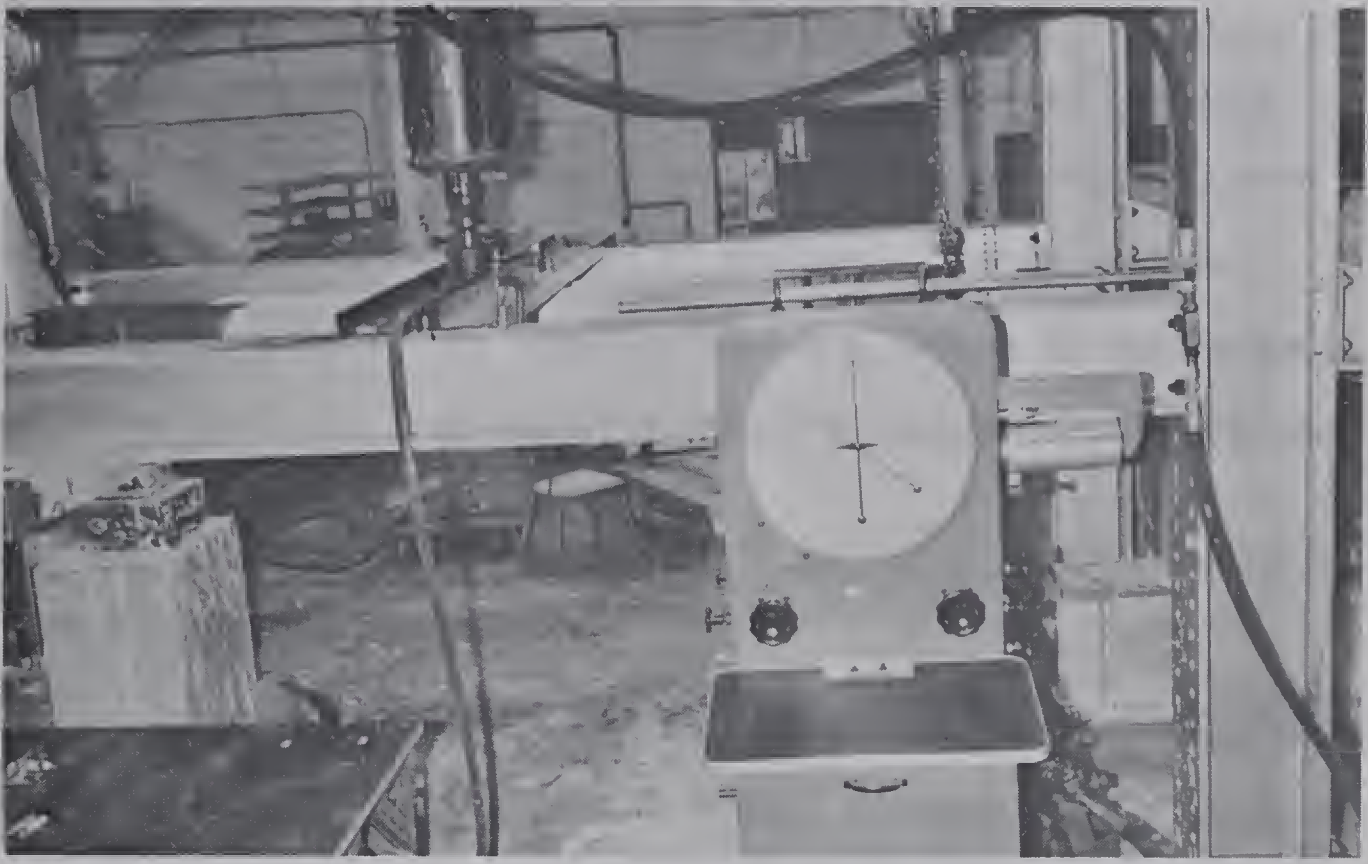

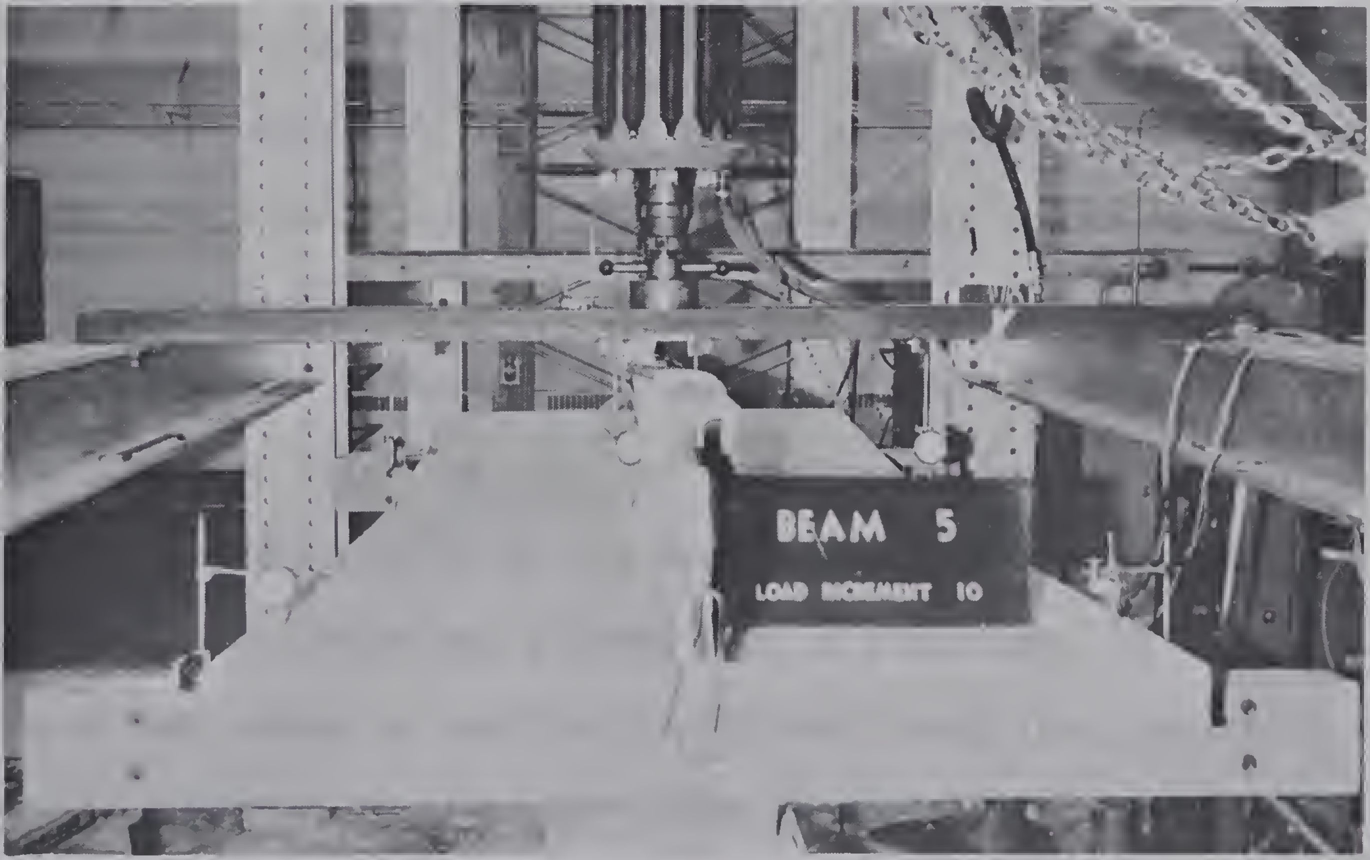

PLATE 3.2 TEST ARRANGEMENT AND BEAM INSTRUMENTATION

on a hinge unit anchored to a concrete pedestal and the other rested on a similar hinge unit mounted on a roller assembly.

Lateral support was provided for the head of the jack. This was accomplished by means of an 8-inch channel with a 6-inch diameter hole cut through the web at midspan. The channel was placed transversely to the beam specimen and bolted to the loading frame. The jack had free travel of about 5-inches through the hole in the channel.

3.7 TEST PROCEDURE

On the day prior to the test, the beam specimen was lifted into place, centered in the loading frame, and seated in plaster of Paris on the transverse support beams. The electrical resistance strain gauges were connected to the strain indicator.

At the beginning of each test, a load of about 200 pounds was applied. Under this load, all gauges were checked and initial readings were taken. Also at this time shrinkage cracks in the concrete were marked.

The load increments were either determined before a particular test, or after the previous load increment based on the deflection characteristics of the beam. After the load increment was applied, the system was allowed time to stabilize. At high loads, the specimens tended to continue to deflect slowly at a constant load. When this occurred, readings were taken as soon as the rate of deflection became constant. Cracks were marked at each load increment following the taking of readings.

The first tests were terminated as soon as the applied load could not be increased. In later tests load was reduced to stabilize the beam in an attempt to obtain readings for the descending portion of the load-deflection curve. This procedure proved difficult, and only limited success was achieved.

CHAPTER IV

TEST RESULTS

4.1 INTRODUCTION

All original data obtained from the beam tests is filed in the Department of Civil Engineering, University of Alberta. Much of this data is presented herein principally in graphical form.

4.2 DEFLECTIONS

Centerline deflections of the steel beam section of the composite beam are presented in the form LOAD VS DEFLECTION in FIGURES 4.1, 4.2, and 4.3. FIGURES 4.1 and 4.2 present the same data. However, in FIGURE 4.2 the vertical scale has been non-dimensionalized by use of the load to computed plastic moment capacity load ratio (P/P_p). The method of computing the plastic moment capacity is that recommended by Slutter and Driscoll[4].

The deflection of the edges of the concrete slab and the steel beam section are compared in FIGURE 4.4, COMPARISON OF EDGE AND CENTERLINE DEFLECTIONS.

4.3 END ROTATION DATA

Centerline moments and end rotation data is presented in FIGURES 4.5, 4.6 and 4.7. For FIGURE 4.6 the moment to computed

plastic moment capacity ratio (M/M_p) is used to non-dimensionalize the vertical scale. In these figures, as in all other references to moment, the weight of the beam has been ignored.

4.4 STEEL BEAM STRAINS

The steel beam section strain readings were converted to curvatures by the following process. The strain readings over the beam depth were plotted to scale for each load increment. A best fit straight line was drawn through these points and the slope of this line was taken as the curvature. All curvature data with the exception of that for Gauge Line #2 of BEAM 2 is presented in FIGURES 4.8, 4.9 and 4.10. The curvature data for Gauge Line #2 of BEAM 2 is presented in FIGURE 4.15. FIGURE 4.9 again uses the non-dimensional (M/M_p) vertical scale.

The depth from the extreme concrete fibre to the neutral axis of the beams was also determined from the same scale plot used to determine curvatures. This data is presented in FIGURES 4.18 and 4.19.

4.5 SLAB REINFORCEMENT STRAINS

Data obtained from sixteen SR4-A7 gauges located on the longitudinal reinforcement of each of BEAMS 1, 2, 3 and 4 is presented in the form of longitudinal strain profiles in FIGURE 4.11. Each point on this plot represents average values abtained from two gauges. For BEAMS 5 and 6 only nine gauges were placed on the

longitudinal reinforcement and data from these gauges is presented in the form of two longitudinal strain profiles and one transverse strain profile for each beam in FIGURE 4.12. The data points on this figure represent the results obtained from one gauge.

The test beams had up to 4 gauges applied to transverse reinforcement. The strain values obtained from these gauges are presented in FIGURE 4.13.

4.6 TABLES AND PLATES

In addition to the test results presented graphically, TABLE 4.1 presents a summary of the ultimate moment capacities of the test beams. TABLE 4.2 presents a summary of data obtained from the slab crack patterns. The actual crack patterns are illustrated in PLATES 4.4, 4.5 and 4.6. Also presented by means of plates are the condition of the shear connectors of BEAM 3 after failure of the beam (PLATE 4.1) and the failure modes encountered in this investigation (PLATES 4.2 and 4.3).

4.7 PRESENTATION OF CALCULATED VALUES

As part of this investigation a computer program was written based on the simplifying assumption that a composite beam in the negative moment region is analogous to the steel beam section subjected to an axial force produced by the longitudinal slab reinforcement. This program produced tables expressing bending moment, position of the neutral axis, steel strains, and force in

the slab reinforcement as functions of the curvature and degree of interaction between the steel section and the slab reinforcement. From these tables were chosen the combination of moment, curvature and position of the neutral axis most closely corresponding to the results obtained experimentally for a particular load increment. The comparisons of calculated and experimental values of moments and curvatures are presented in FIGURES 4.14 to 4.17. Comparisons of calculated and experimental positions of the neutral axis are presented in FIGURES 4.18 and 4.19. Graphs depicting the interaction factors and tension forces corresponding to the calculated values are shown on FIGURES 4.20 to 4.23.

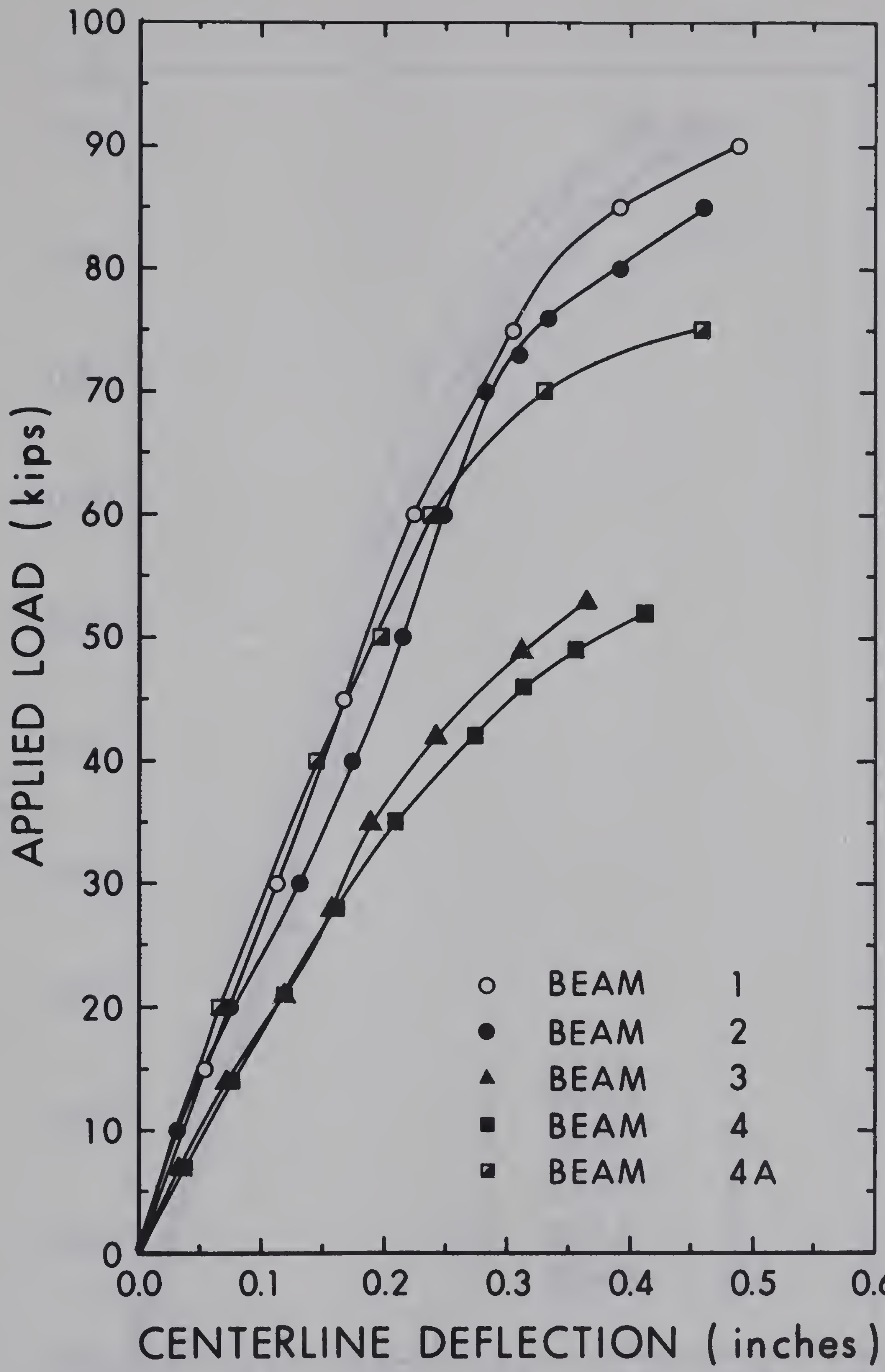

FIGURE 4.1 LOAD VS DEFLECTION

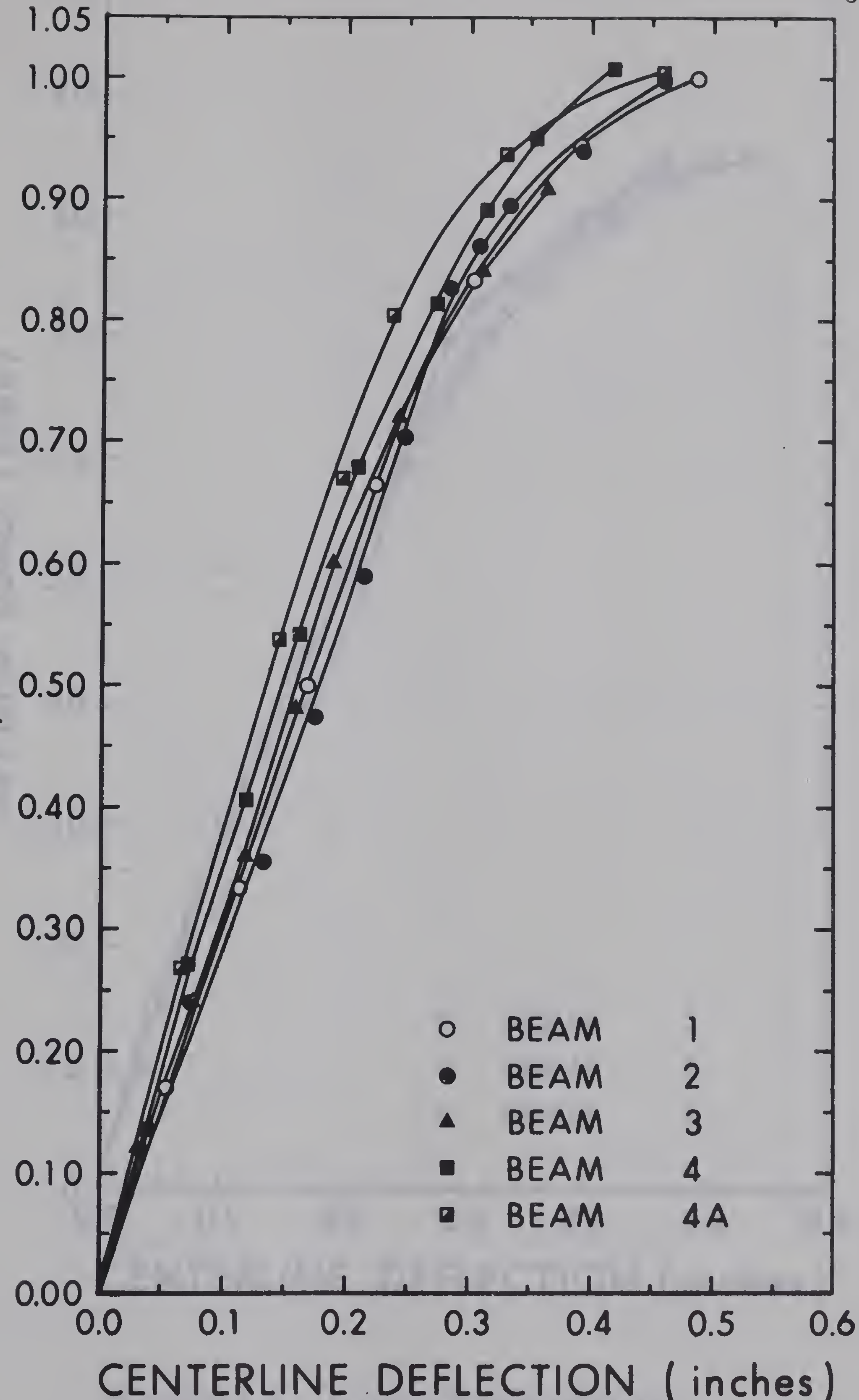

FIGURE 4.2 LOAD VS DEFLECTION

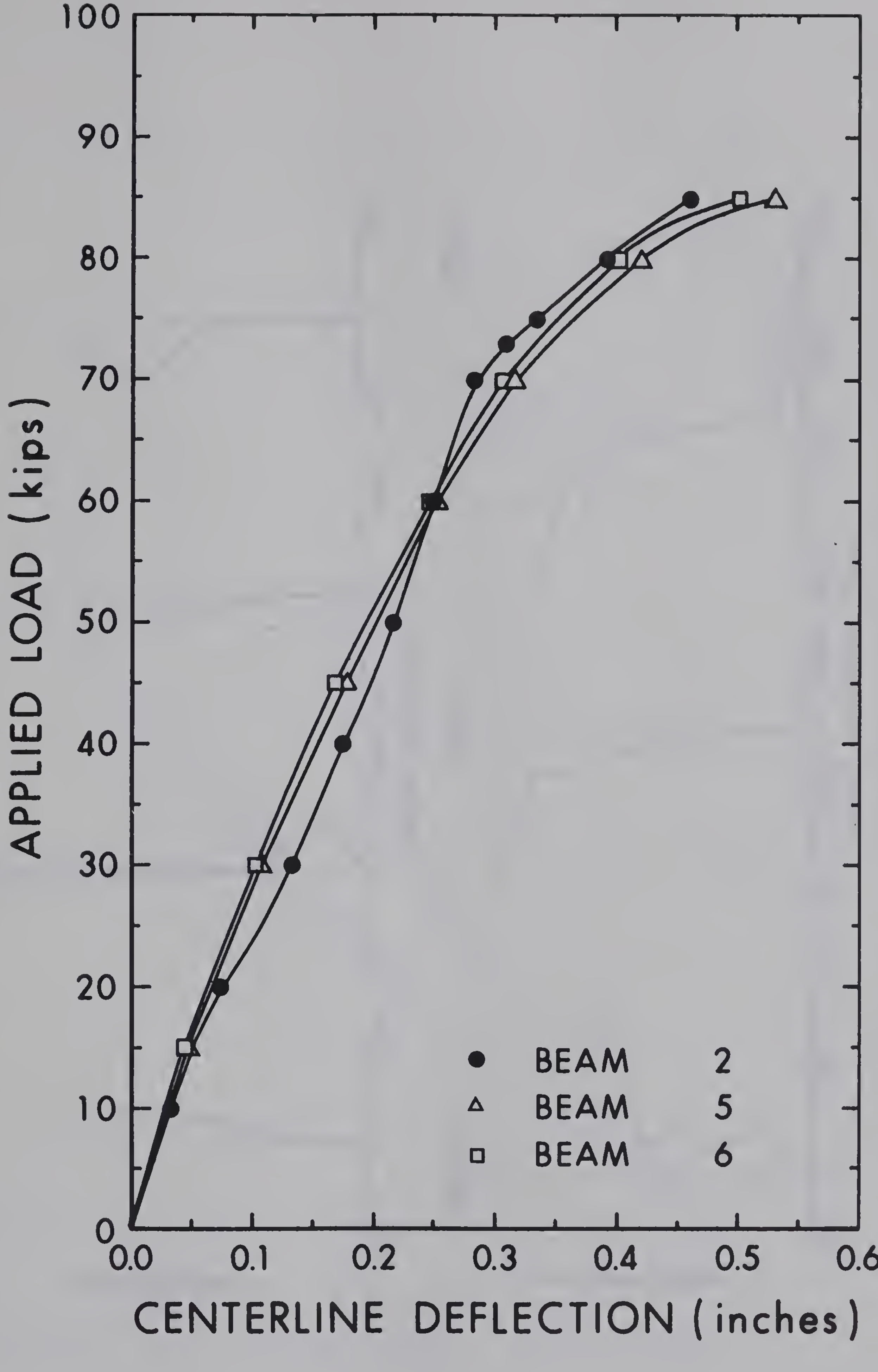

FIGURE 4.3 LOAD VS DEFLECTION

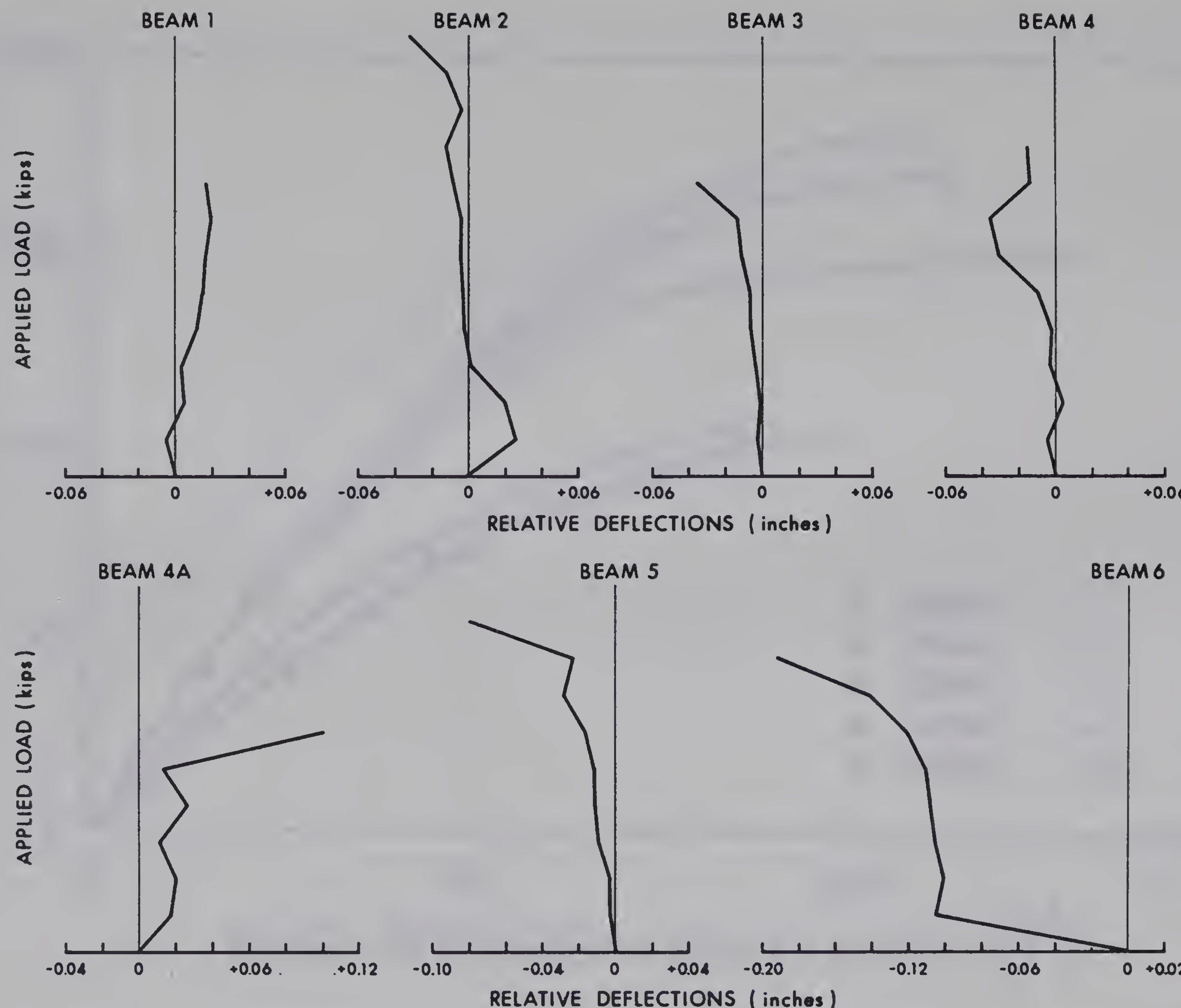

FIGURE 4.4 COMPARISON OF EDGE AND CENTER LINE DEFLECTIONS

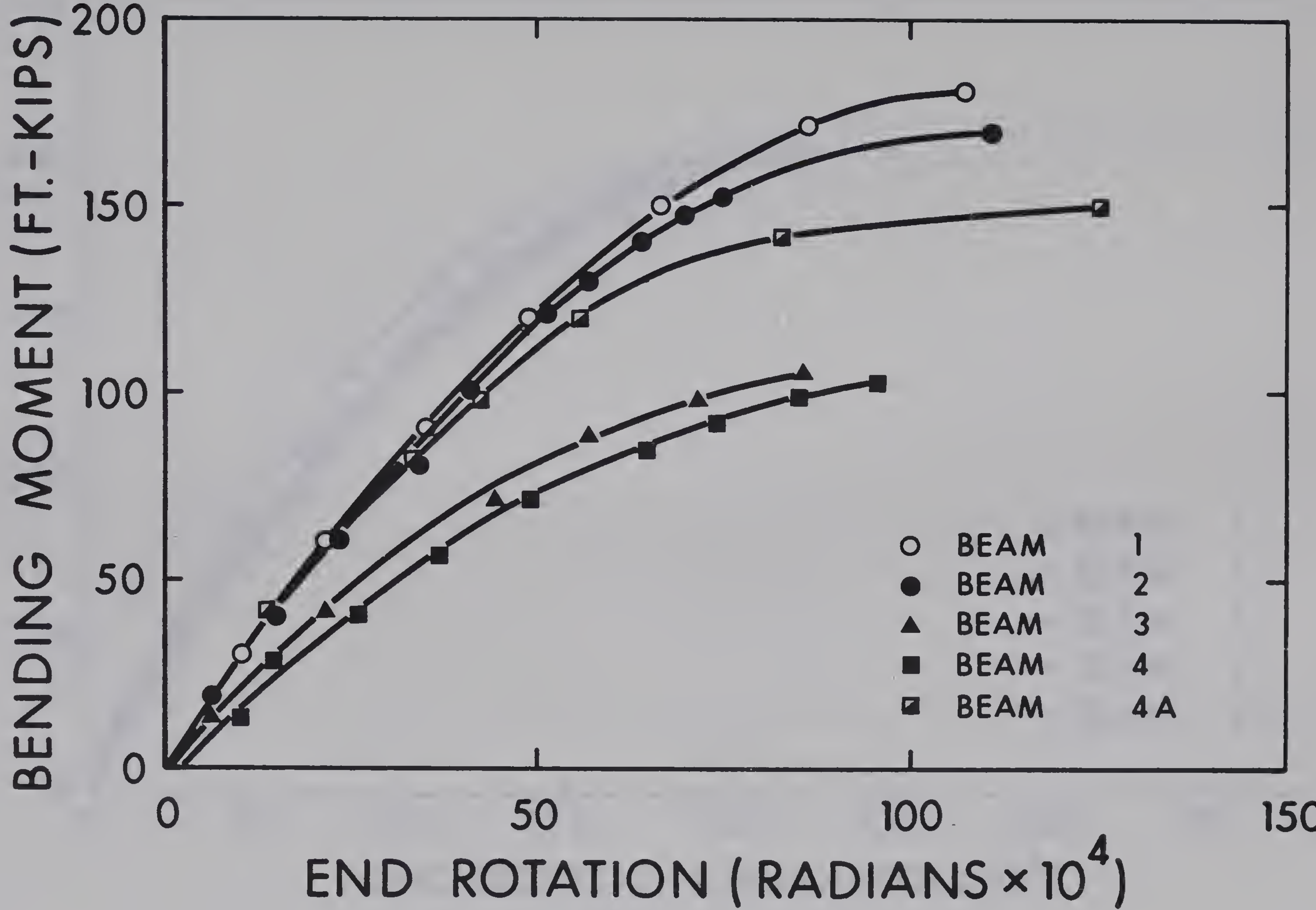

FIGURE 4.5 MOMENT VS END ROTATION

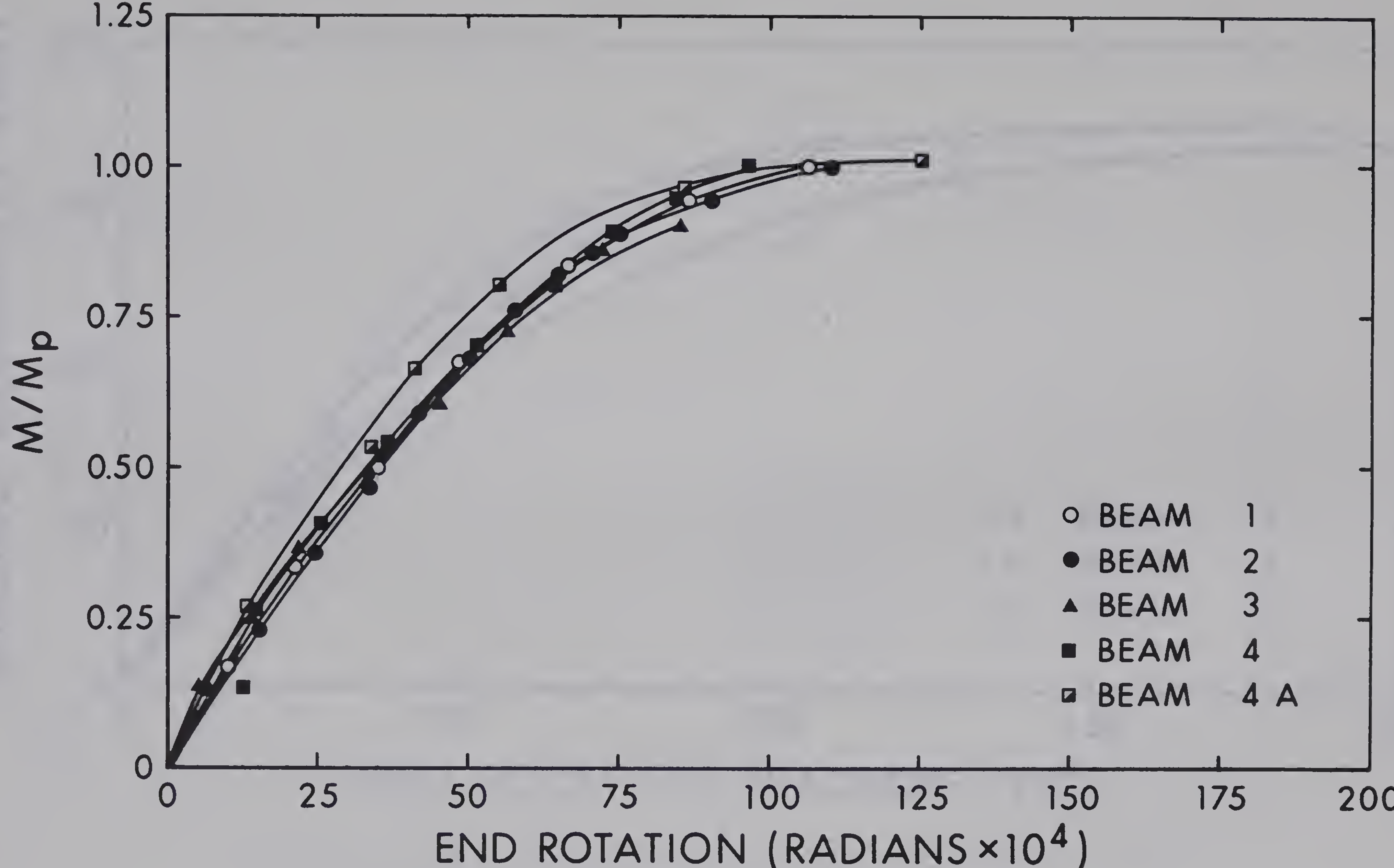

FIGURE 4.6 MOMENT VS END ROTATION

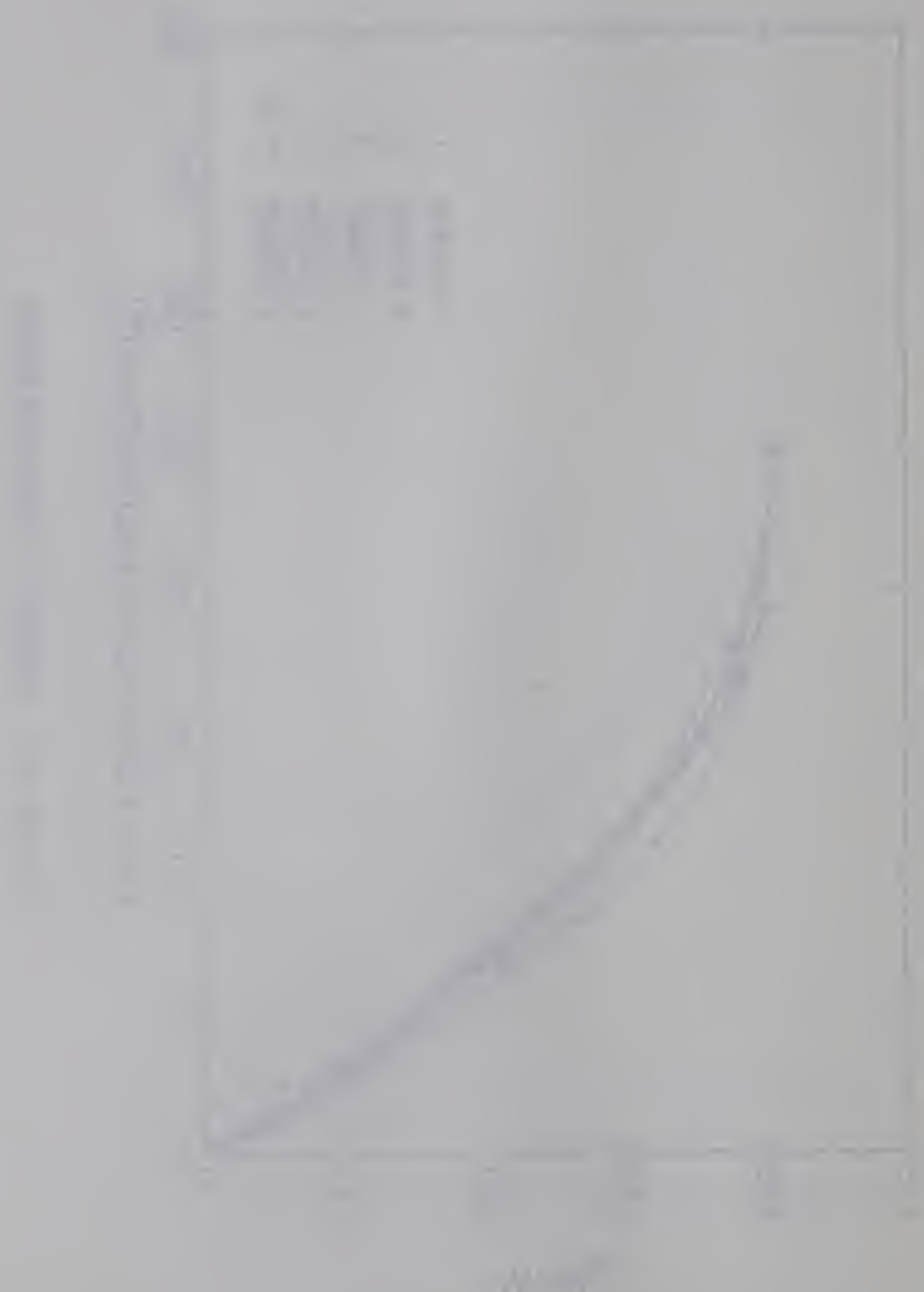

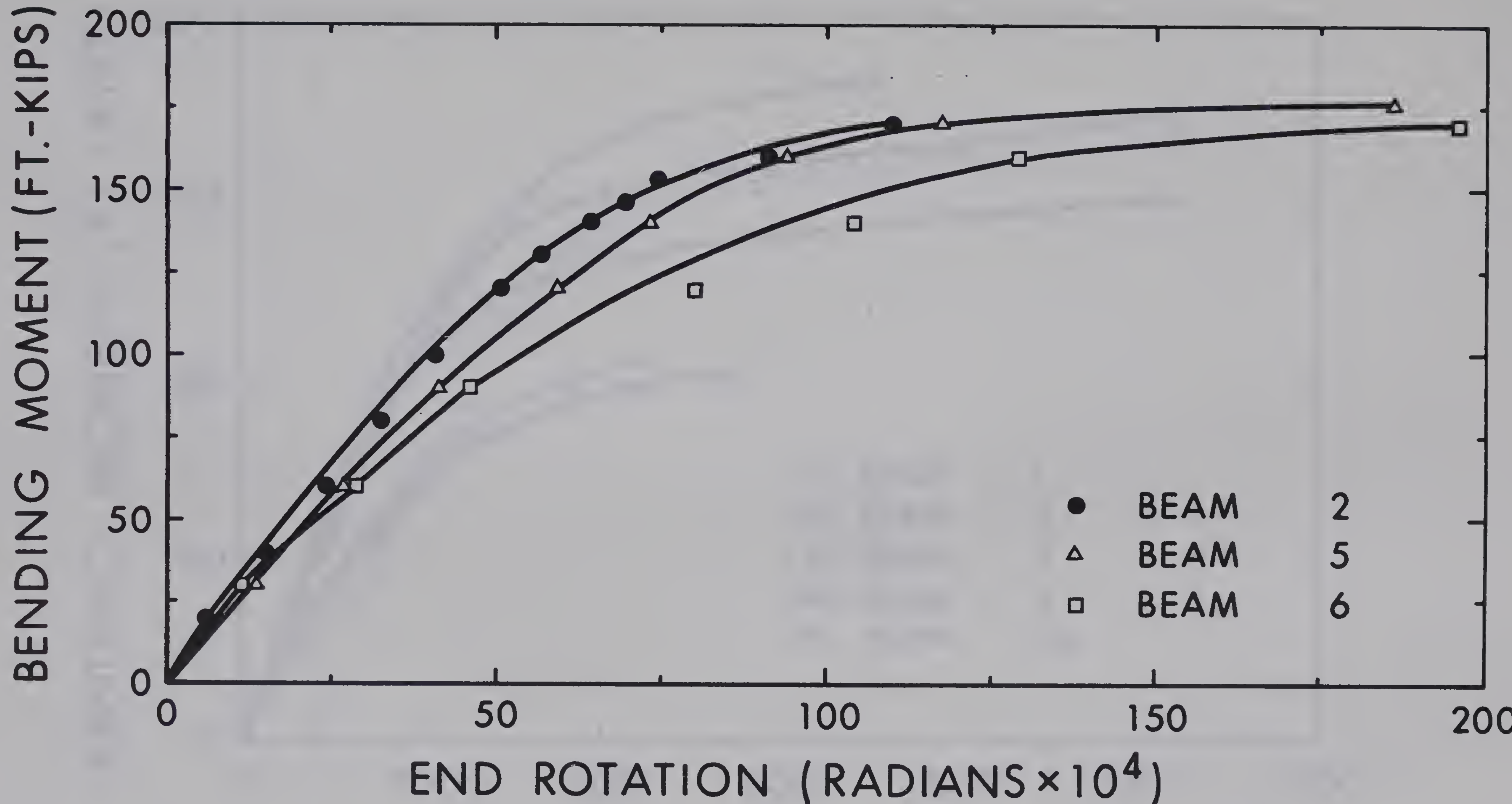

FIGURE 4.7 MOMENT VS END ROTATION

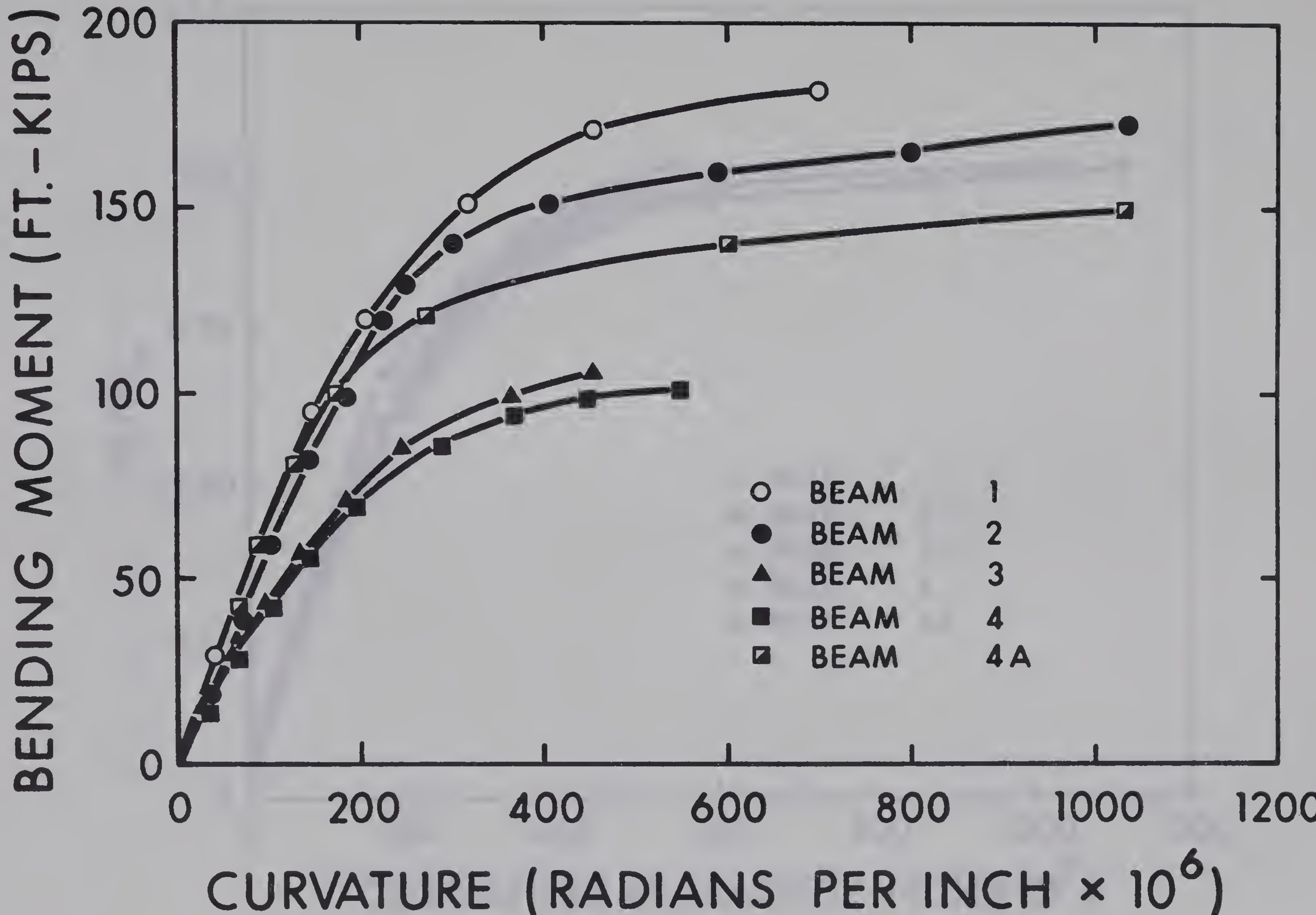

FIGURE 4.8 MOMENT VS CENTER LINE CURVATURE

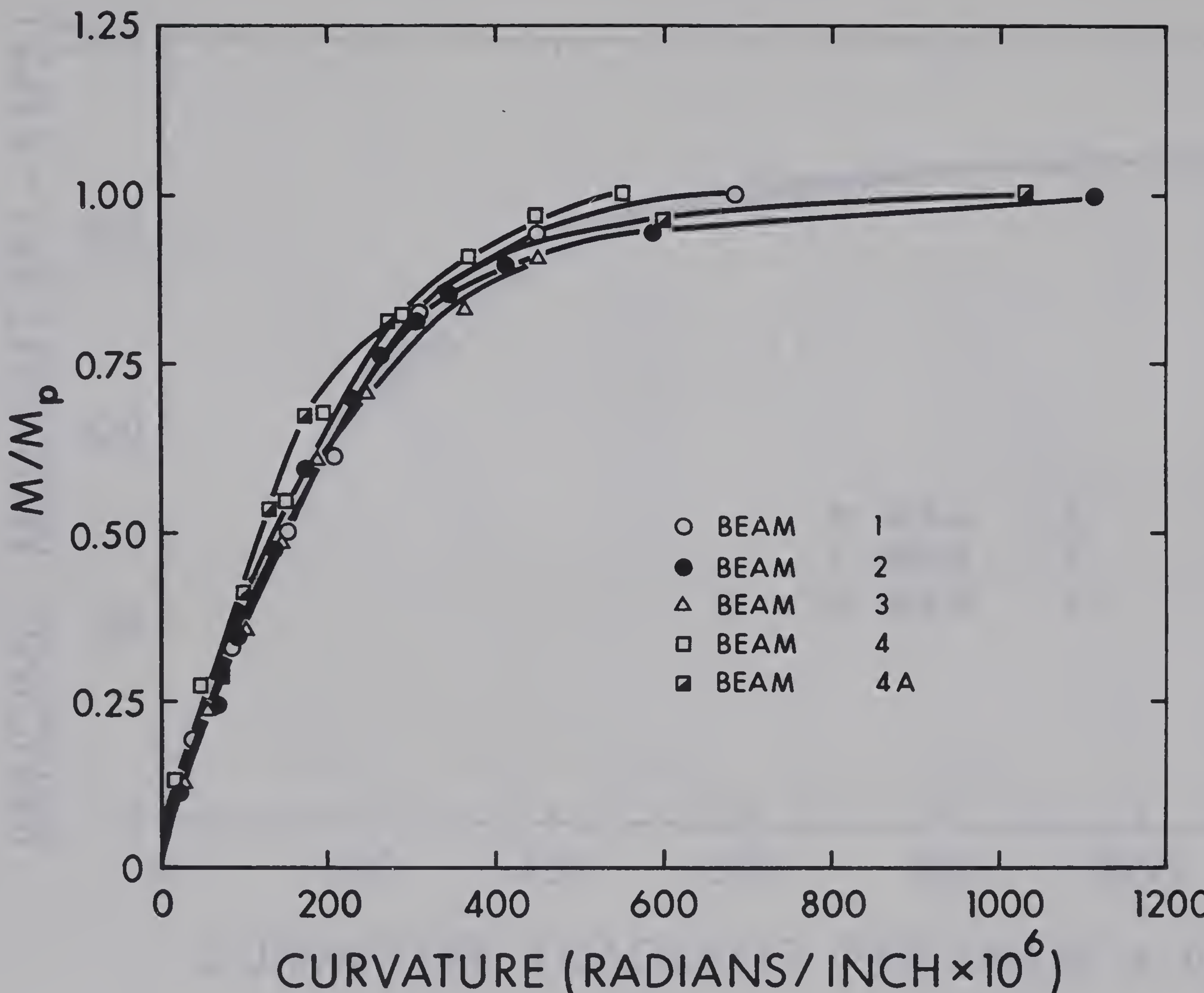

FIGURE 4.9 MOMENT VS CENTER LINE CURVATURE

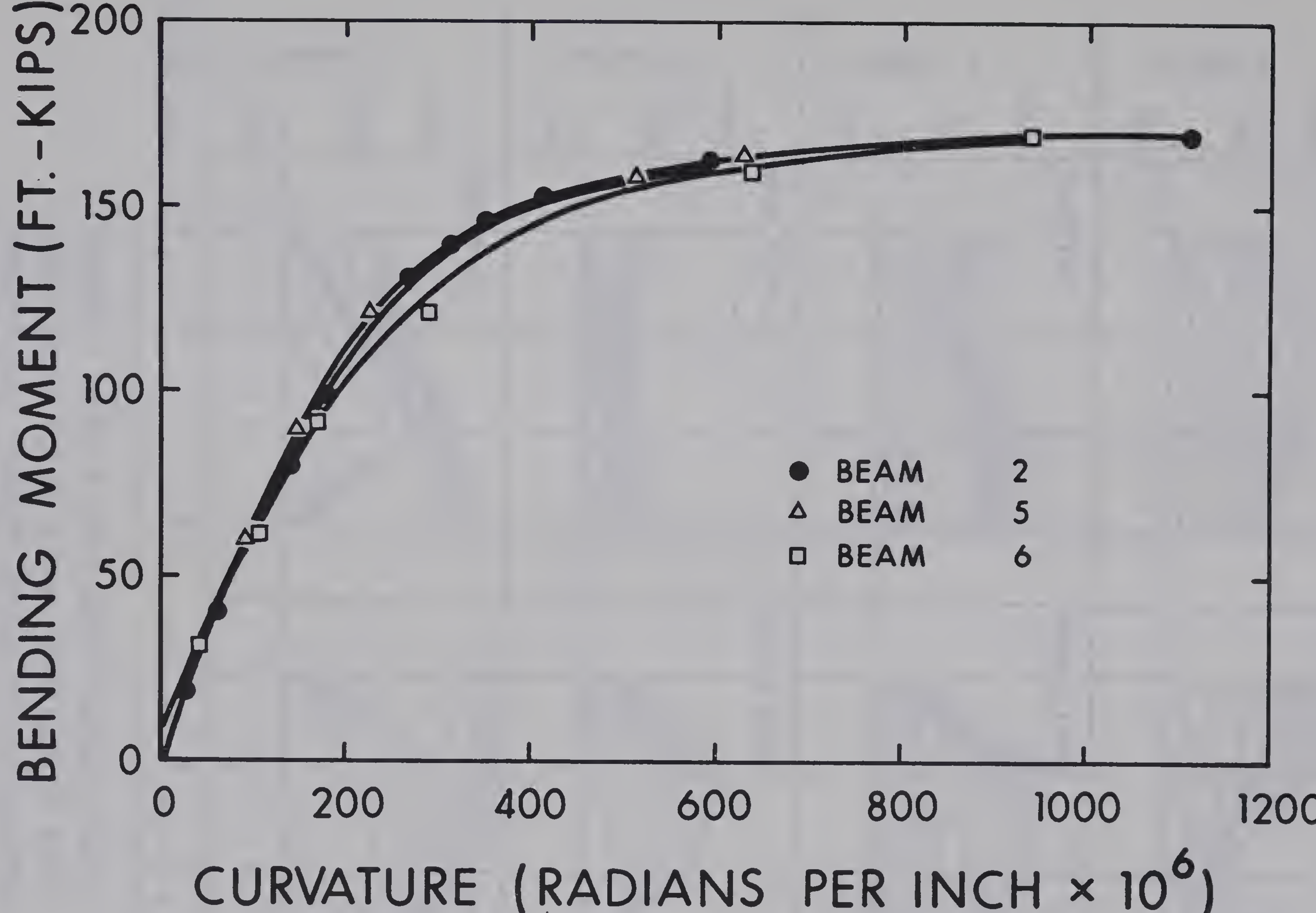

FIGURE 4.10 MOMENT VS CENTER LINE CURVATURE

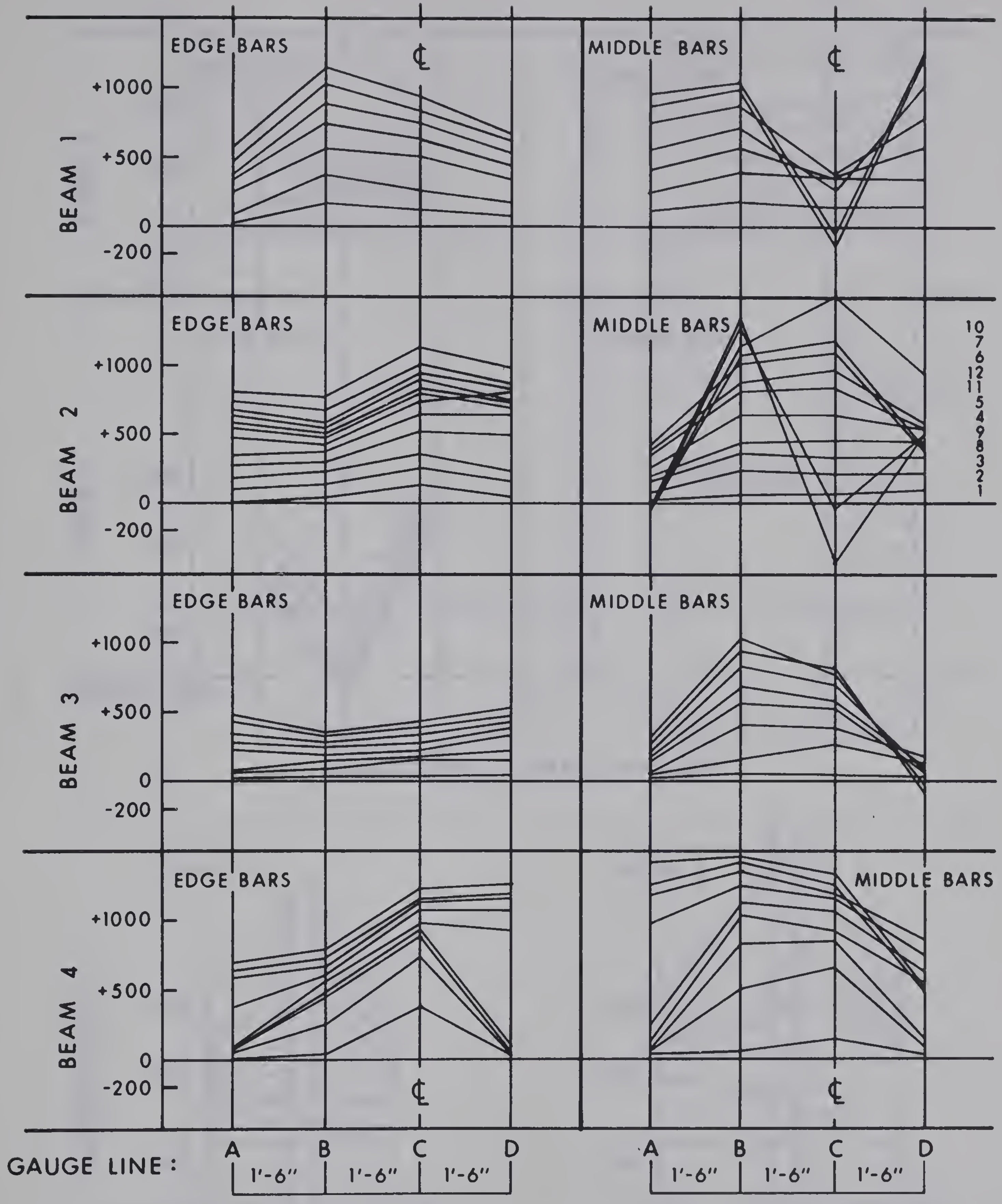

STRAINS: SCALE 1"=1000 MICRO INCHES / INCH

NOTE: EACH POINT IS THE AVERAGE OF TWO SYMETRICALLY PLACED GAGES ON LONGITUDINAL REINFORCING BARS.

FIGURE 4.11 LONGITUDINAL STRAIN PROFILES

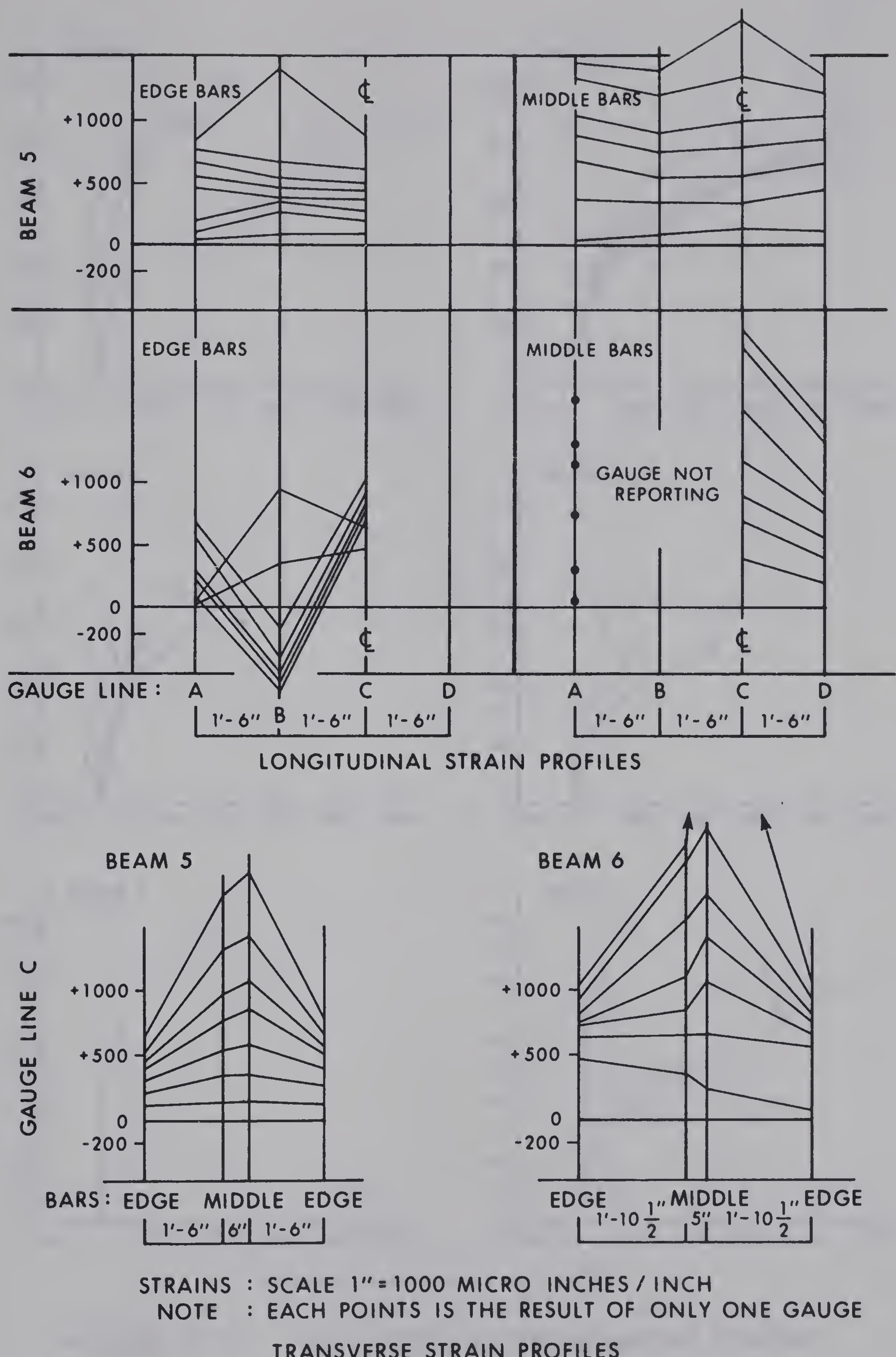

FIGURE 4.12 REINFORCEMENT STRAIN PROFILES

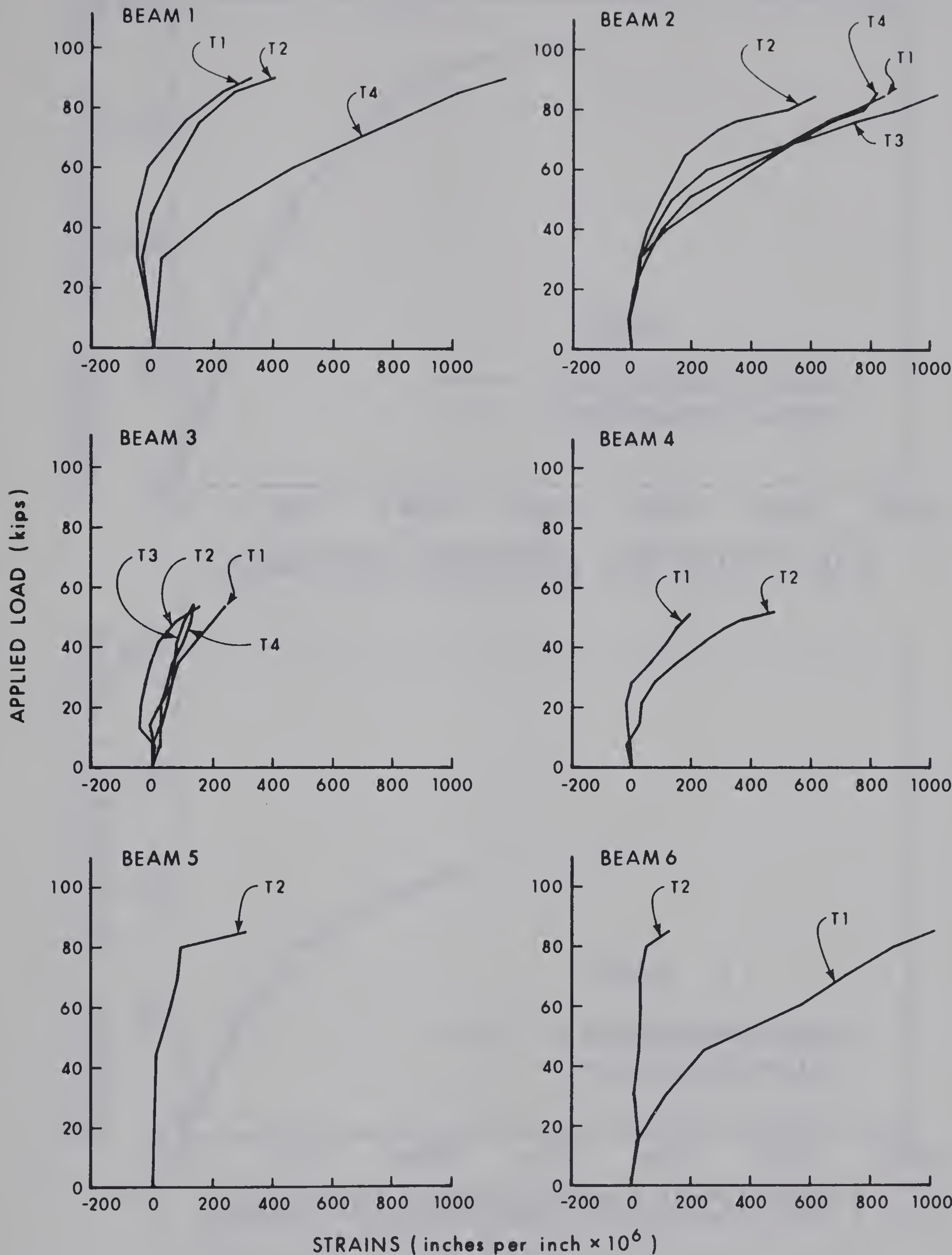

FIGURE 4.13 TRANSVERSE REINFORCEMENT STRAINS

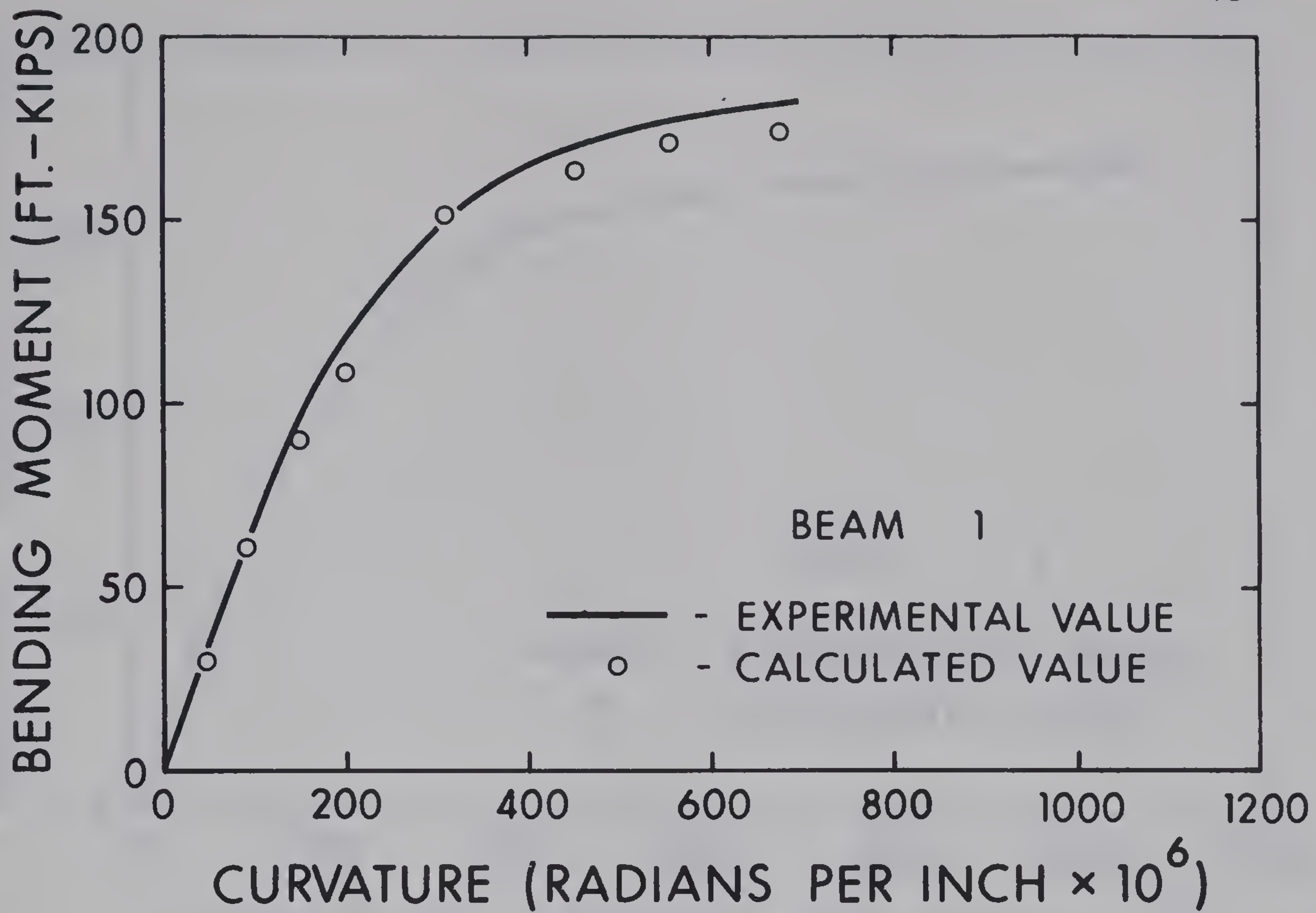

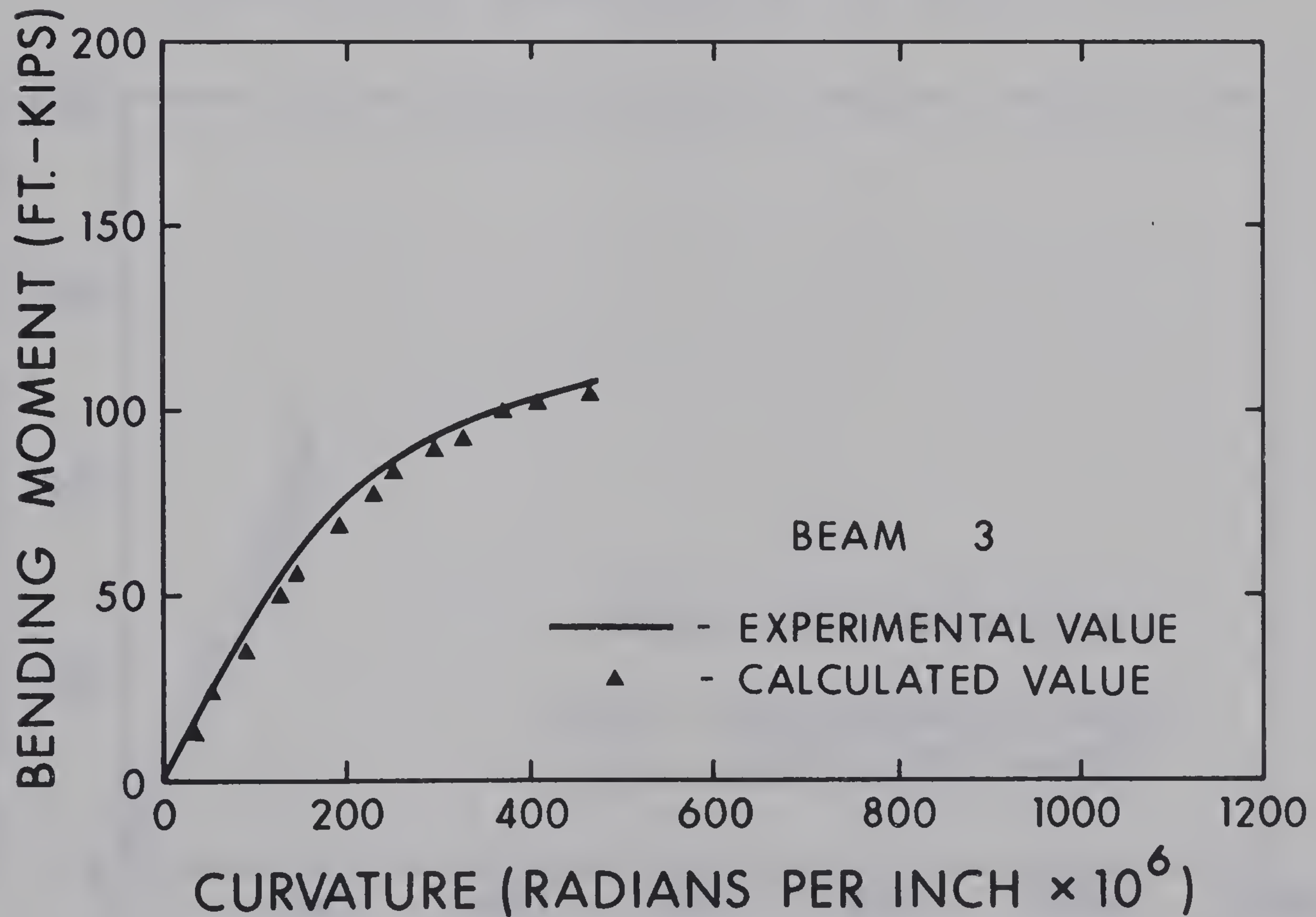

FIGURE 4.14 MOMENT VS CURVATURE

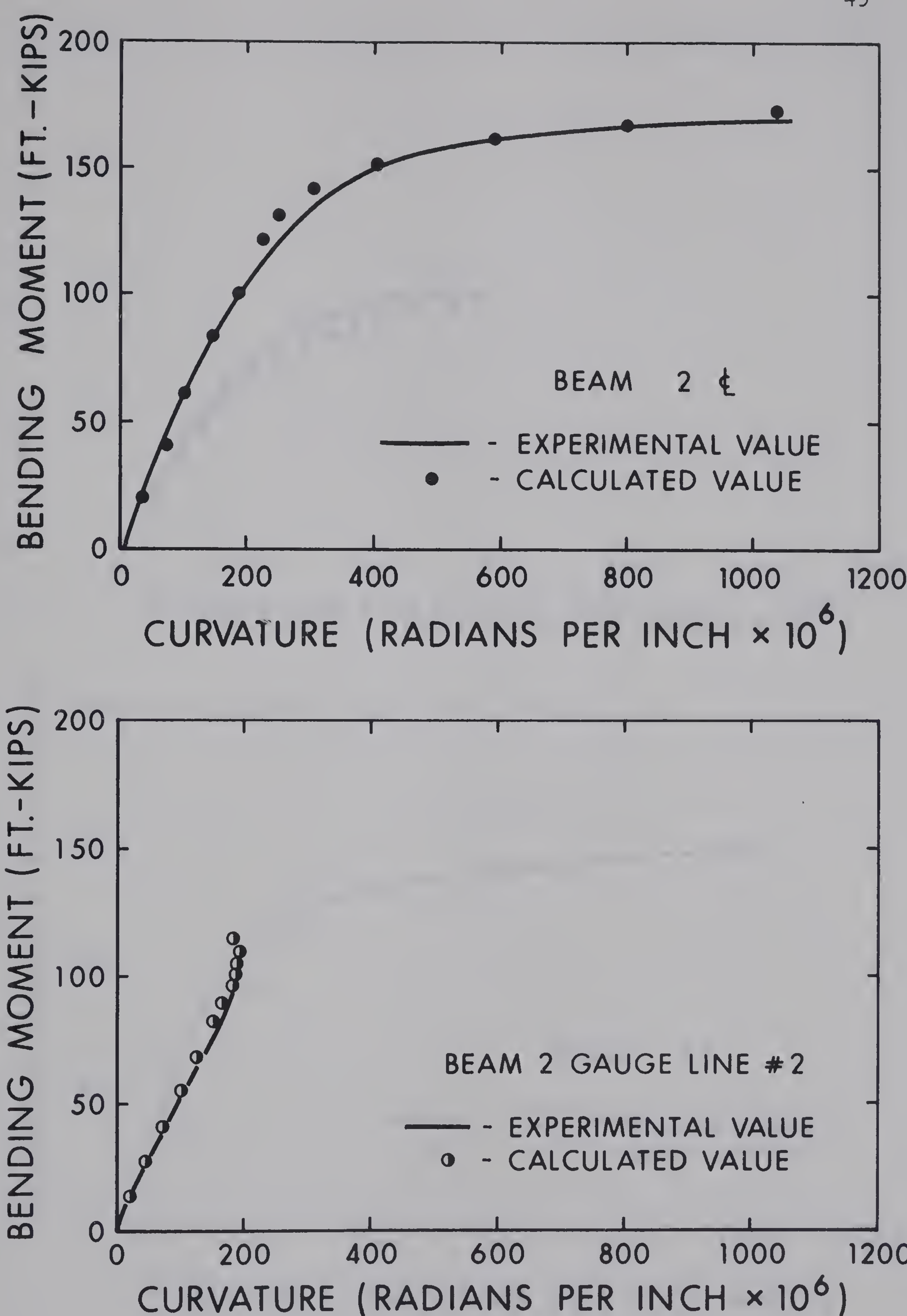

FIGURE 4.15 MOMENT VS CURVATURE

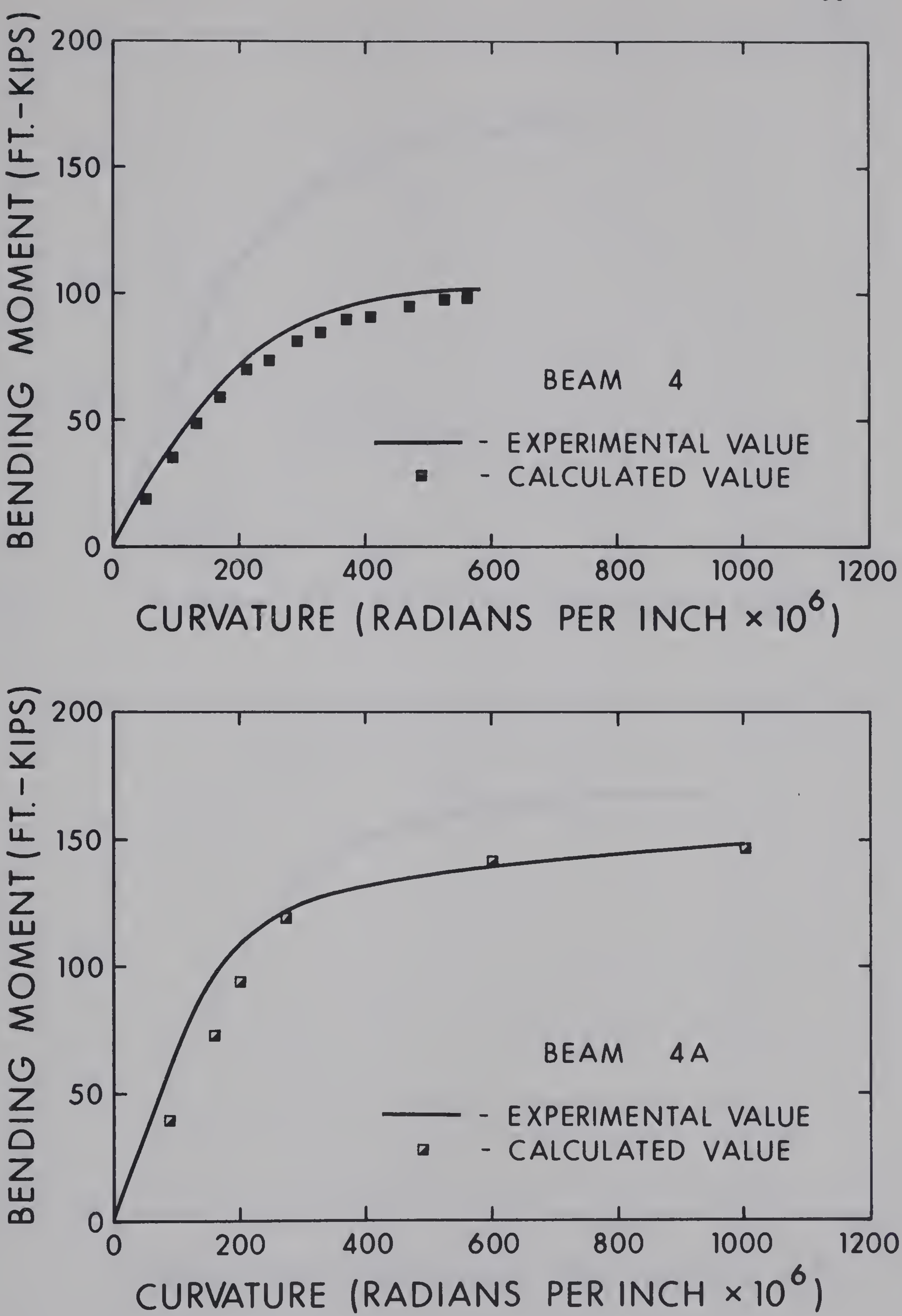

FIGURE 4.16 MOMENT VS CURVATURE

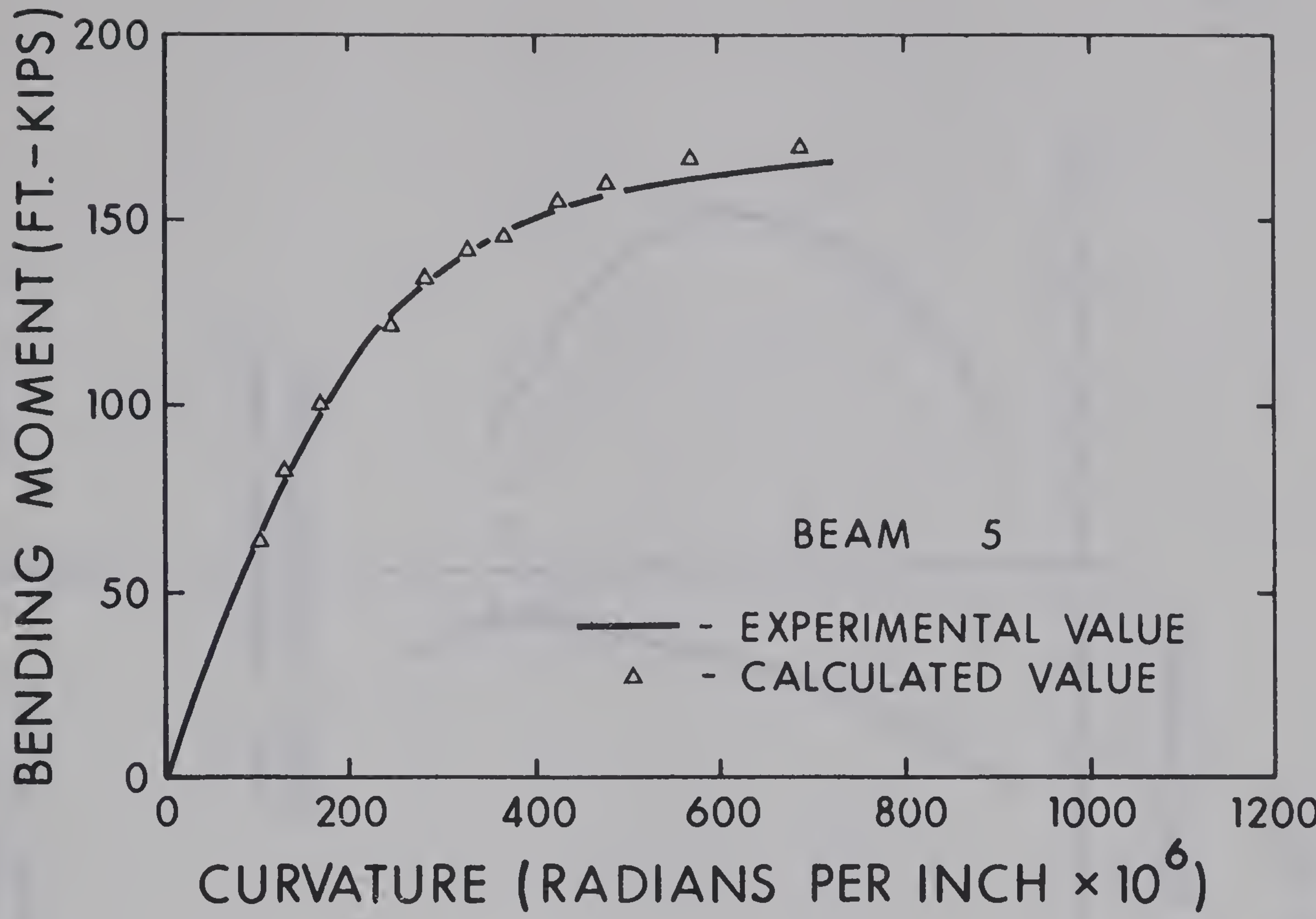

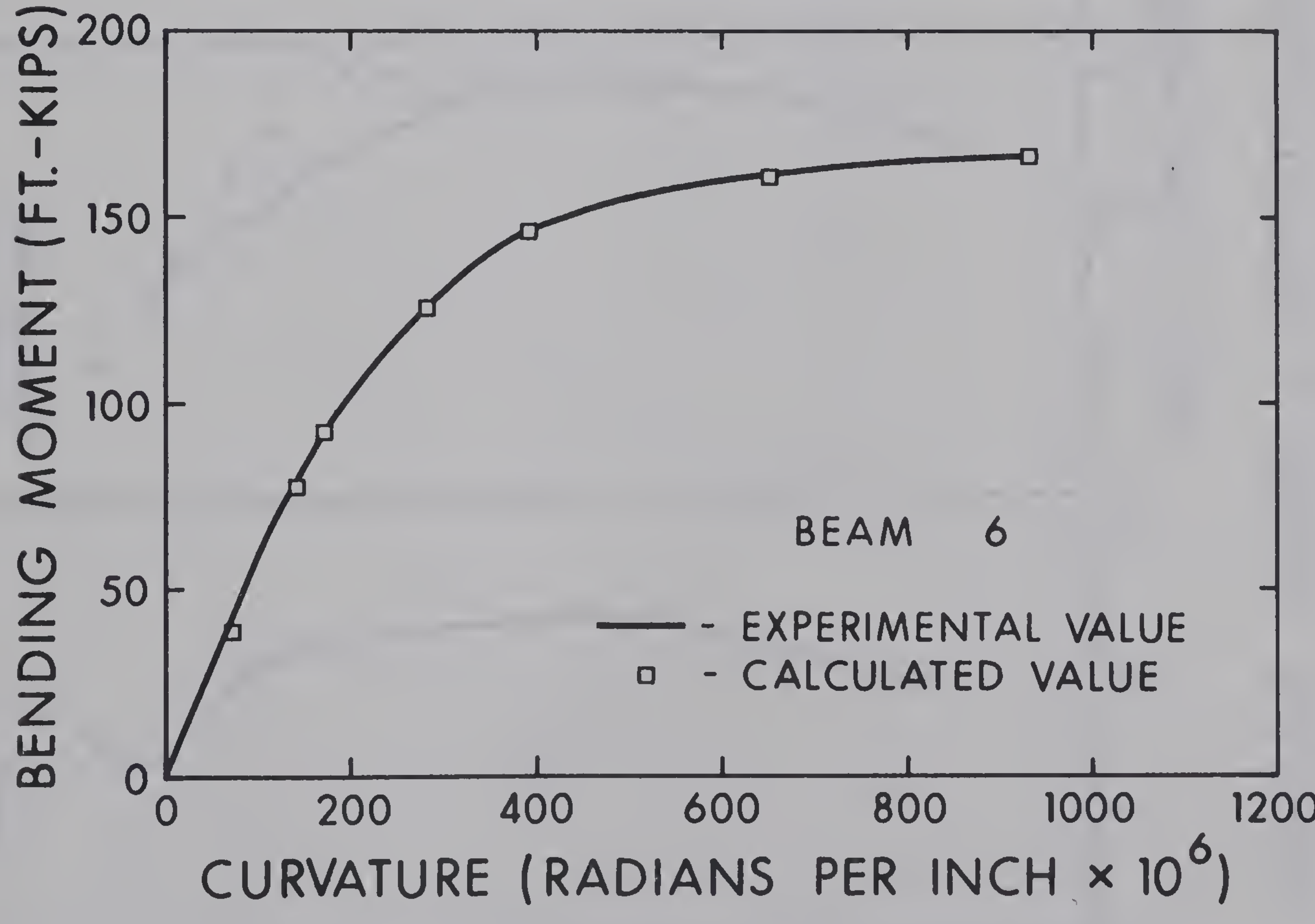

FIGURE 4.17 MOMENT VS CURVATURE

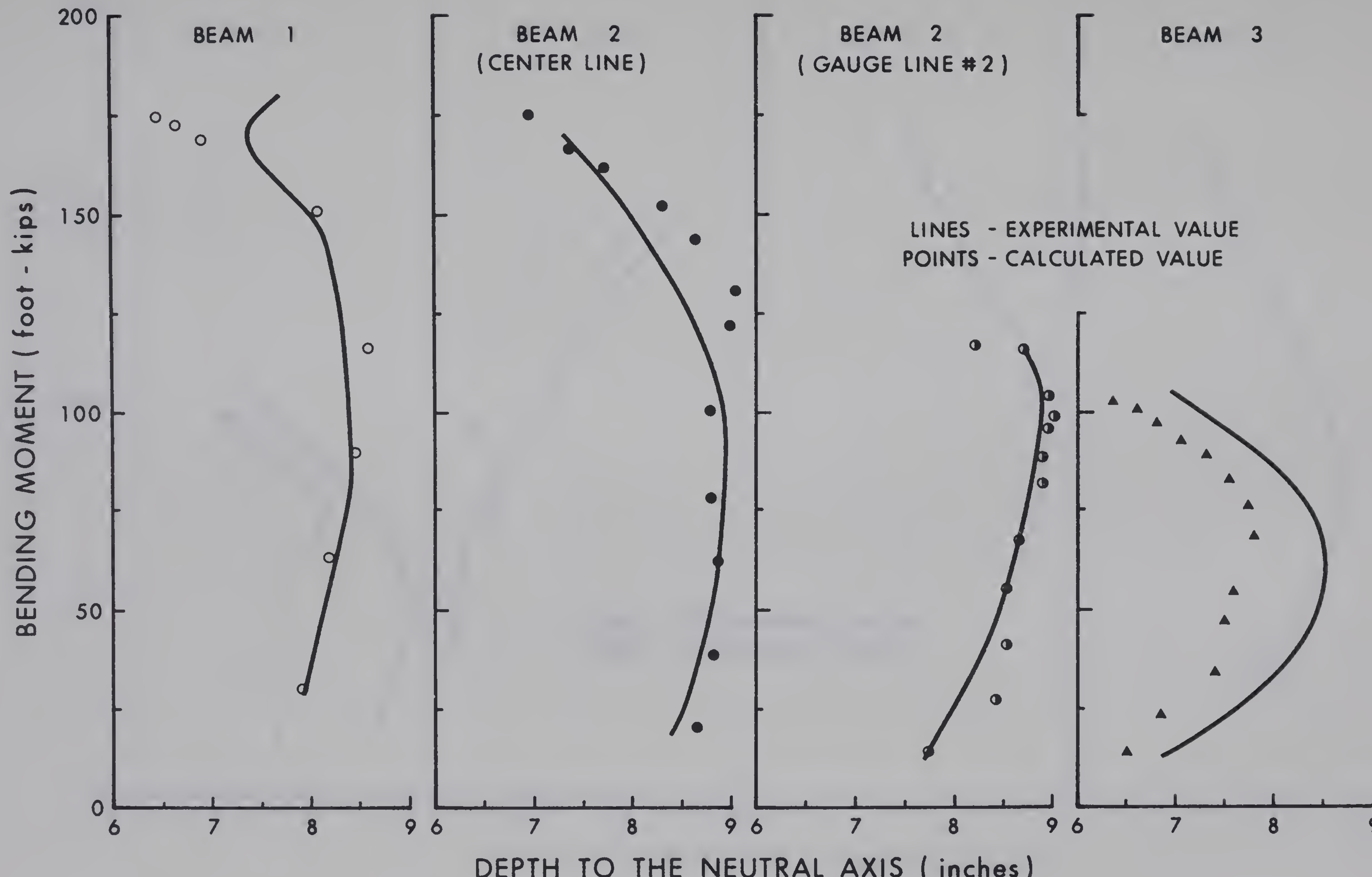

FIGURE 4.18 MOMENT VS DEPTH TO NEUTRAL AXIS

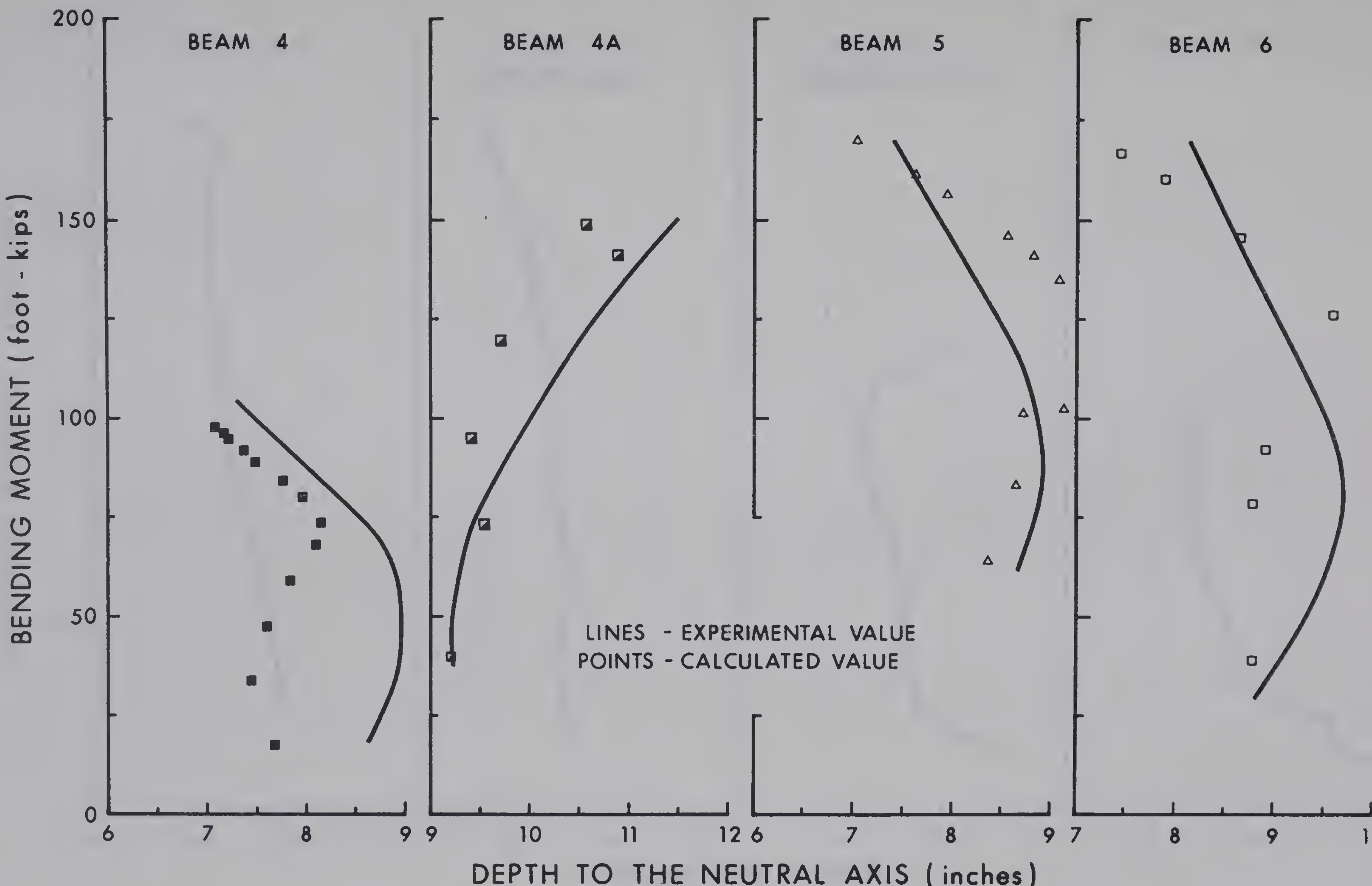

FIGURE 4.19 MOMENT VS DEPTH TO NEUTRAL AXIS

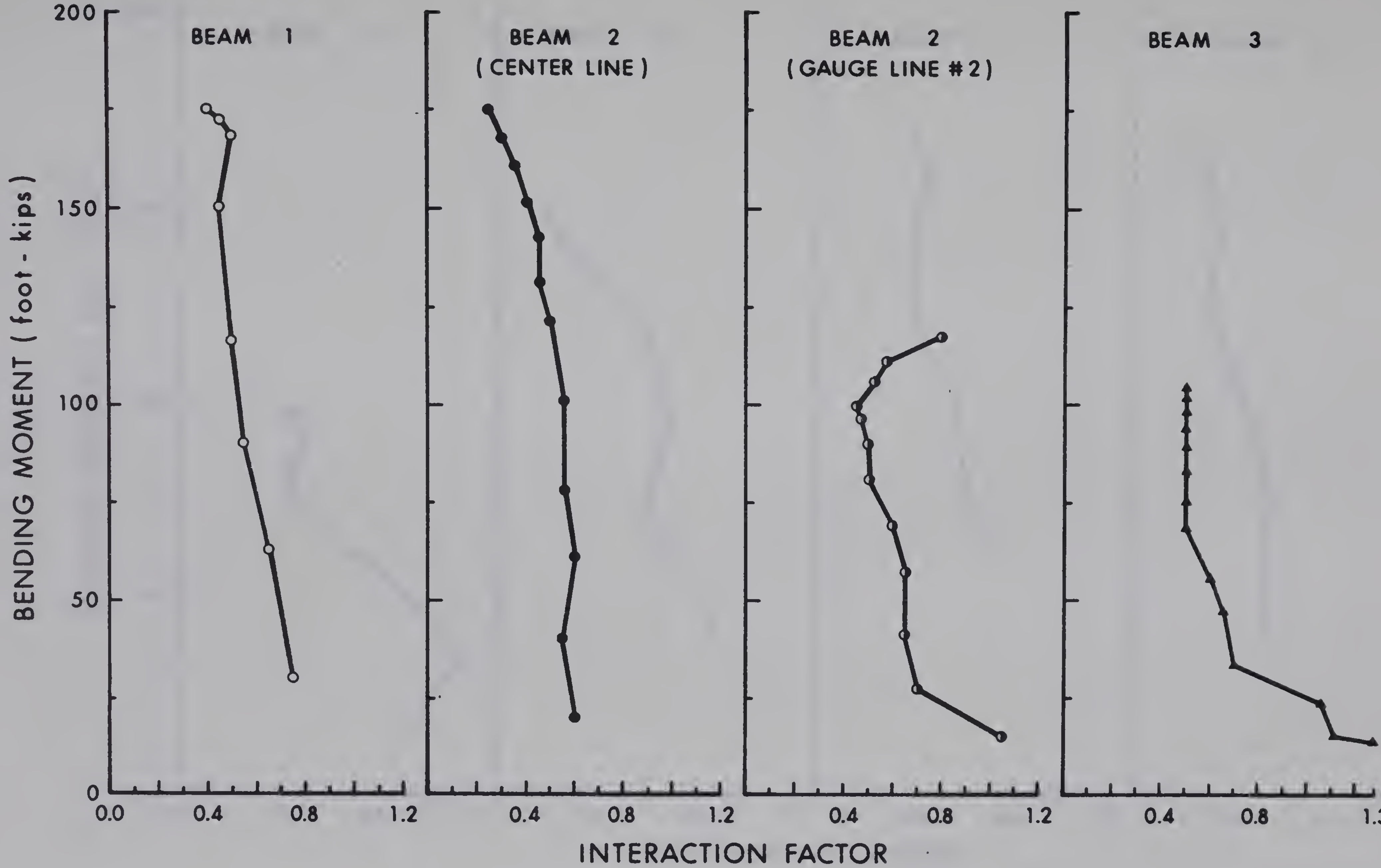

FIGURE 4.20 MOMENT VS INTERACTION FACTOR

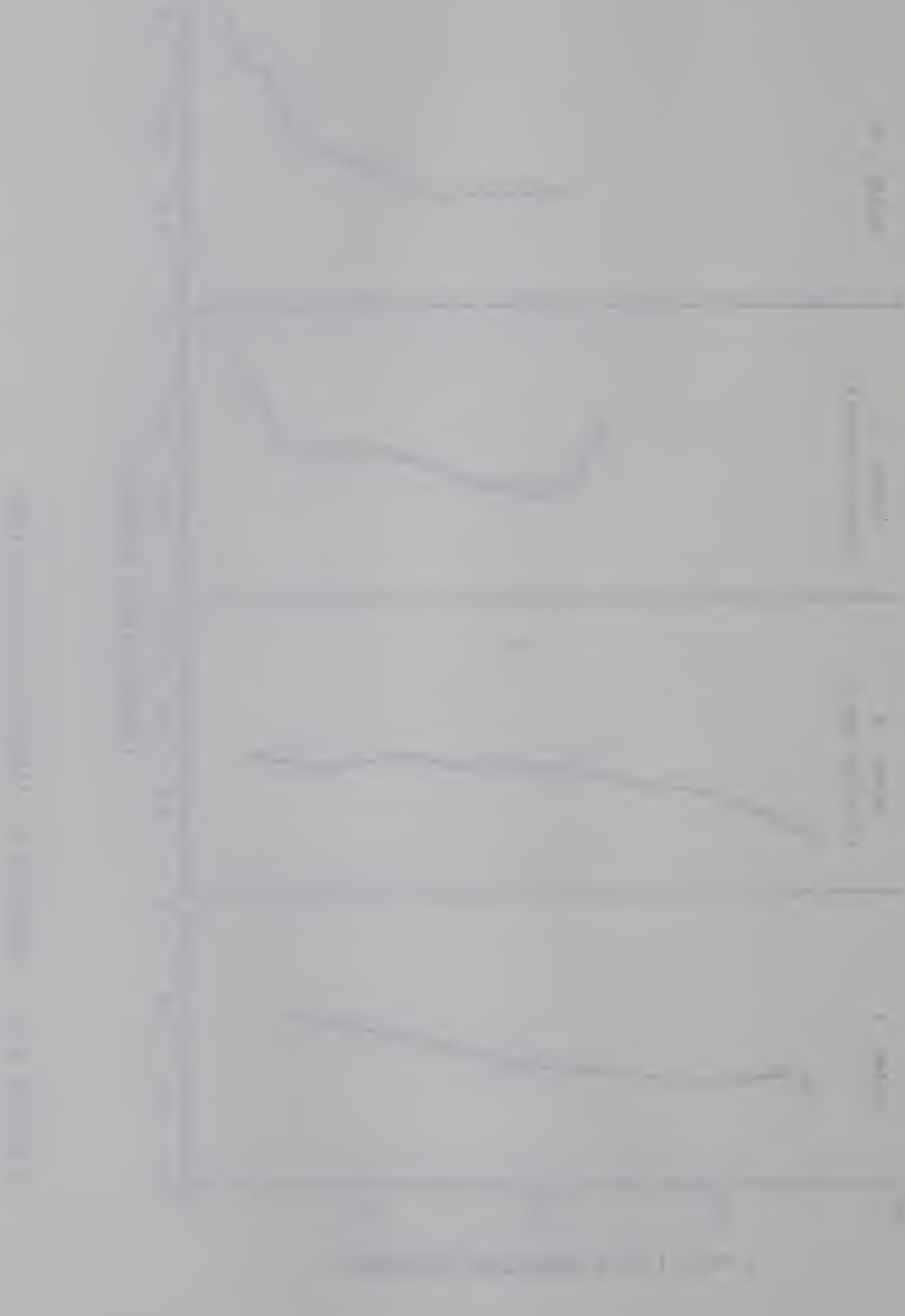

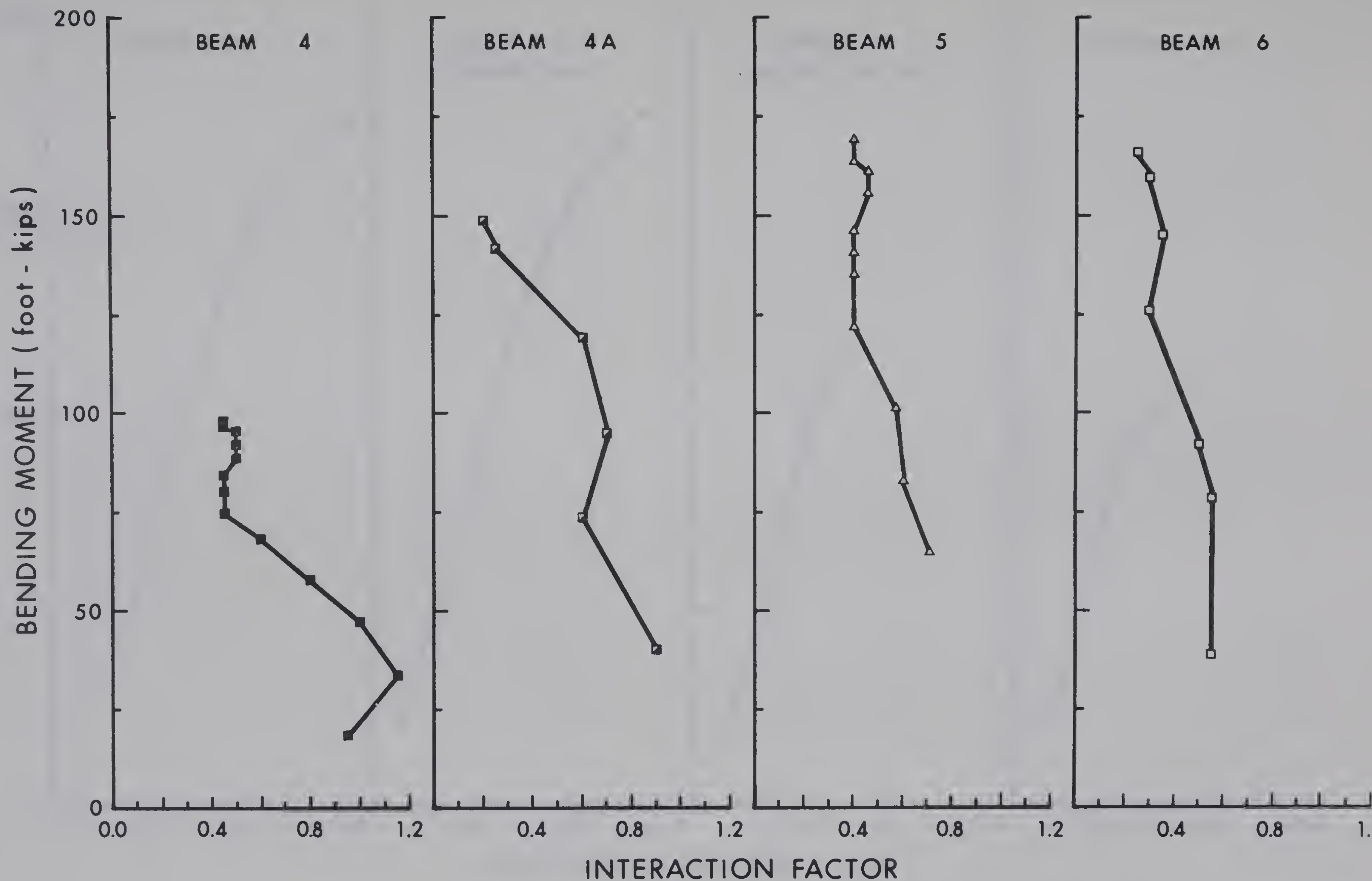

FIGURE 4.21 MOMENT VS INTERACTION FACTOR

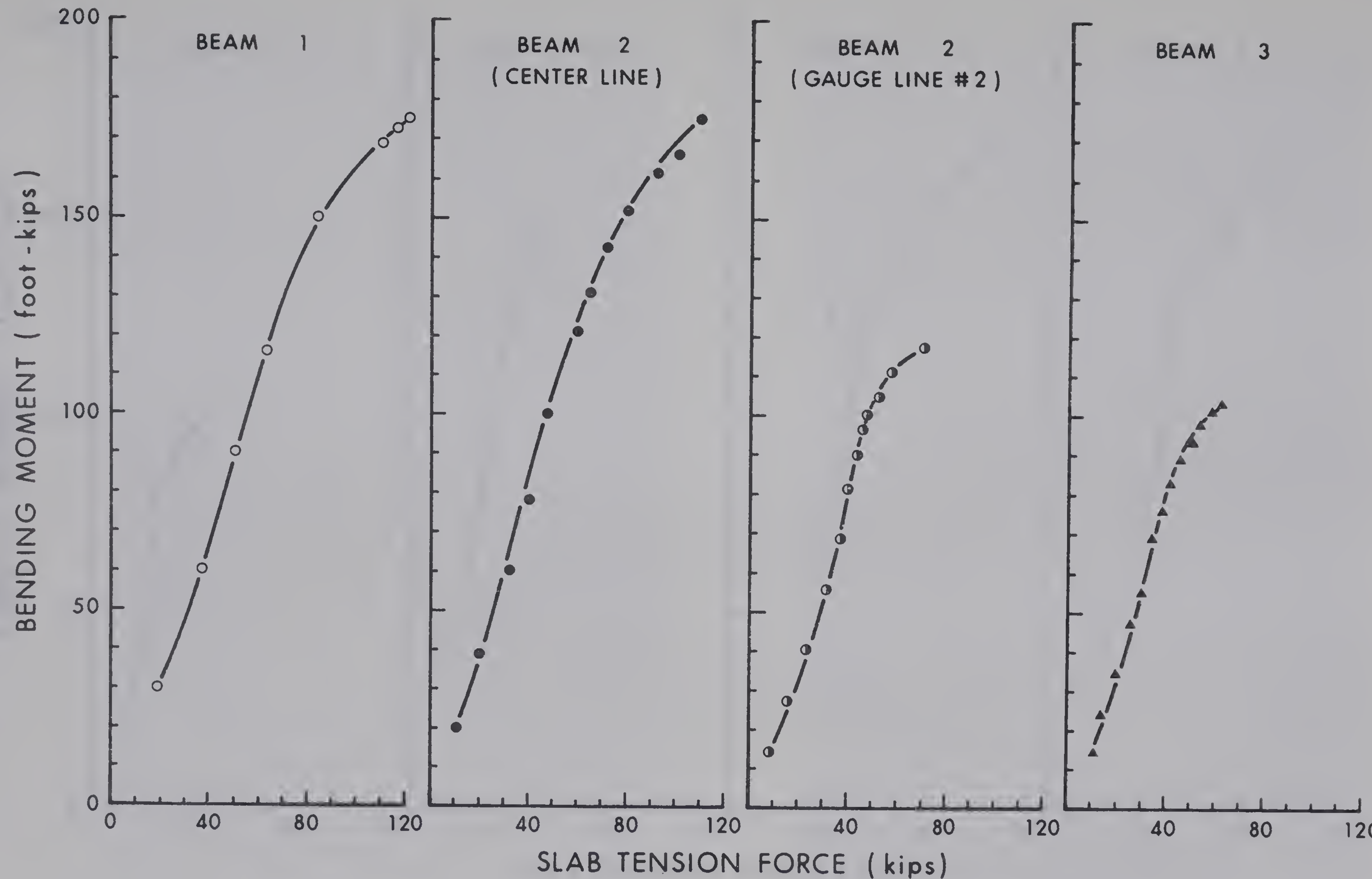

FIGURE 4.22 MOMENT VS TENSION FORCE

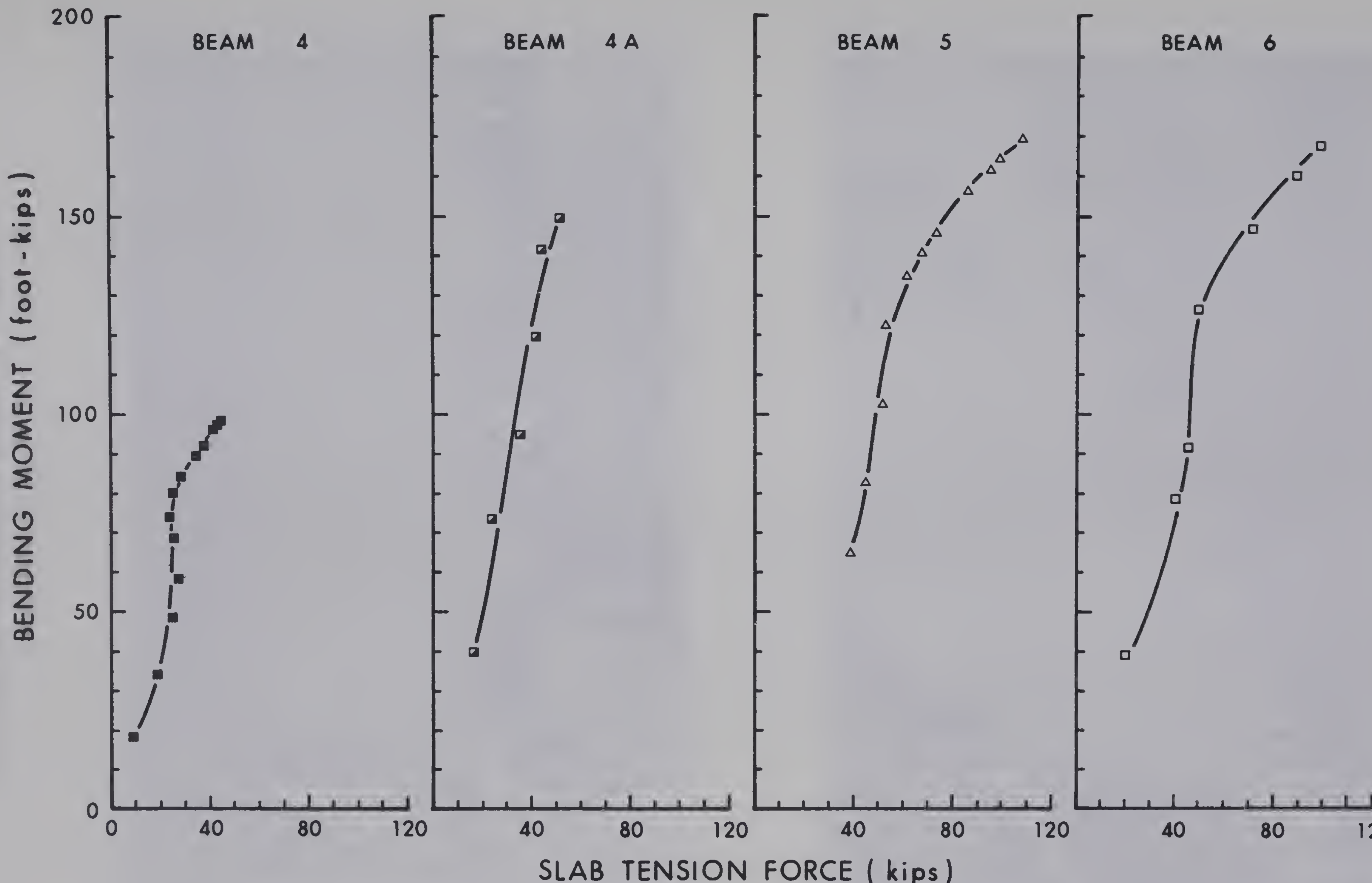

FIGURE 4.23 MOMENT VS TENSION FORCE

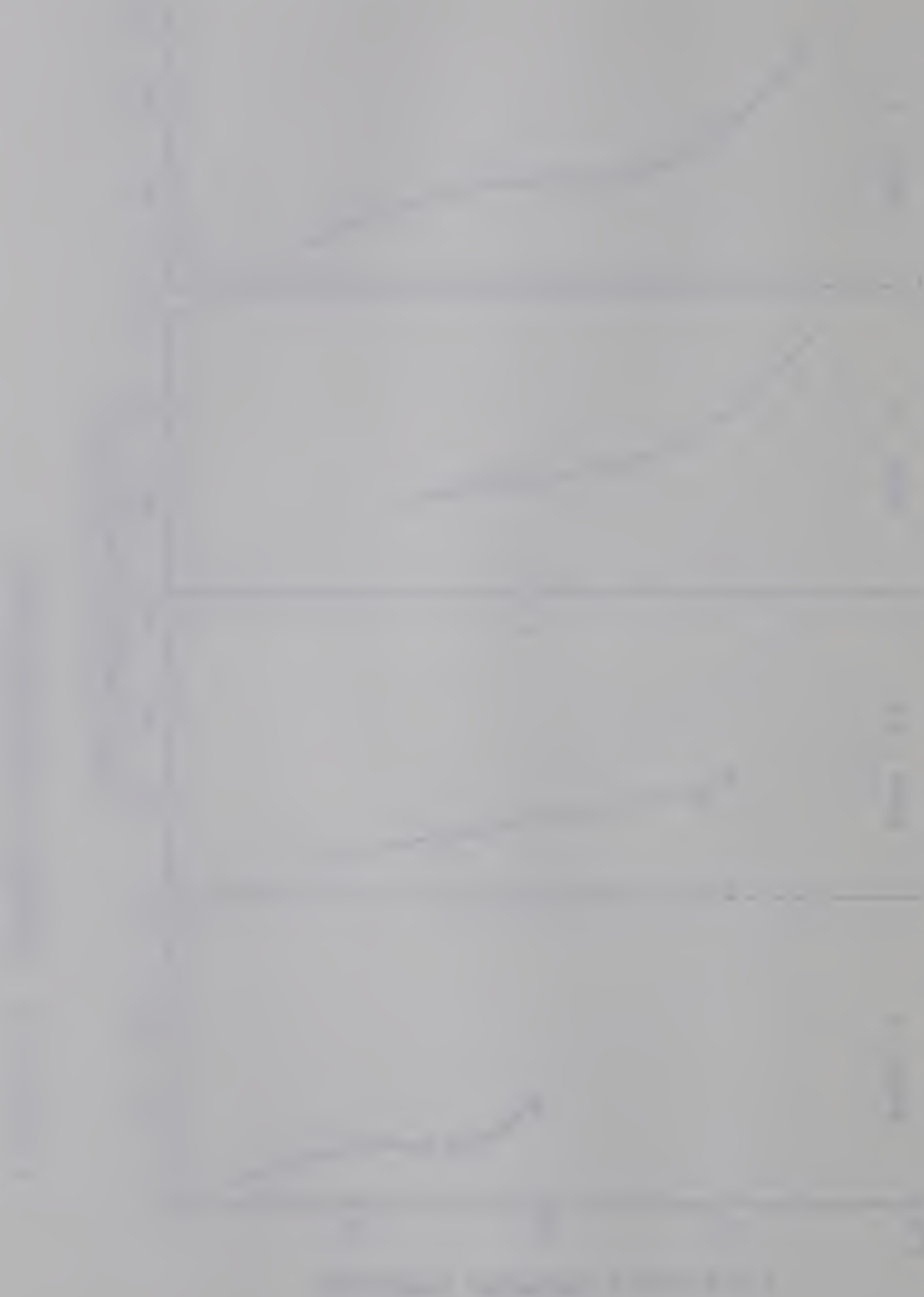

PLATE 4.1 SHEAR CONNECTORS AFTER TEST

(a) LOCAL BUCKLE OF BEAM 4

(b) LOCAL BUCKLE OF BEAM 2

PLATE 4.2 FAILURE MODES

LATERAL BUCKLE OF BEAM 5

PLATE 4.3 FAILURE MODES

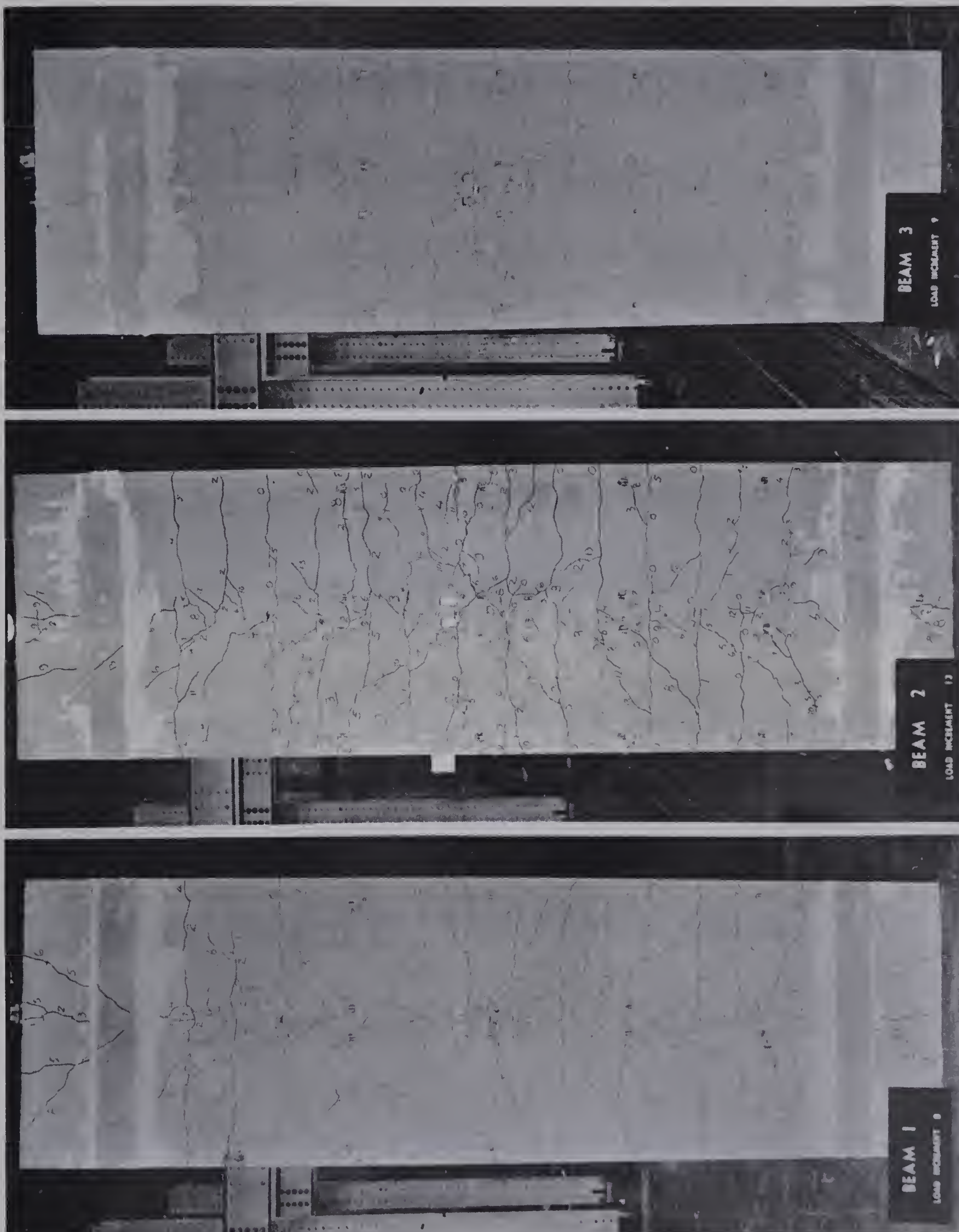

PLATE 4.4 CRACK PATTERNS

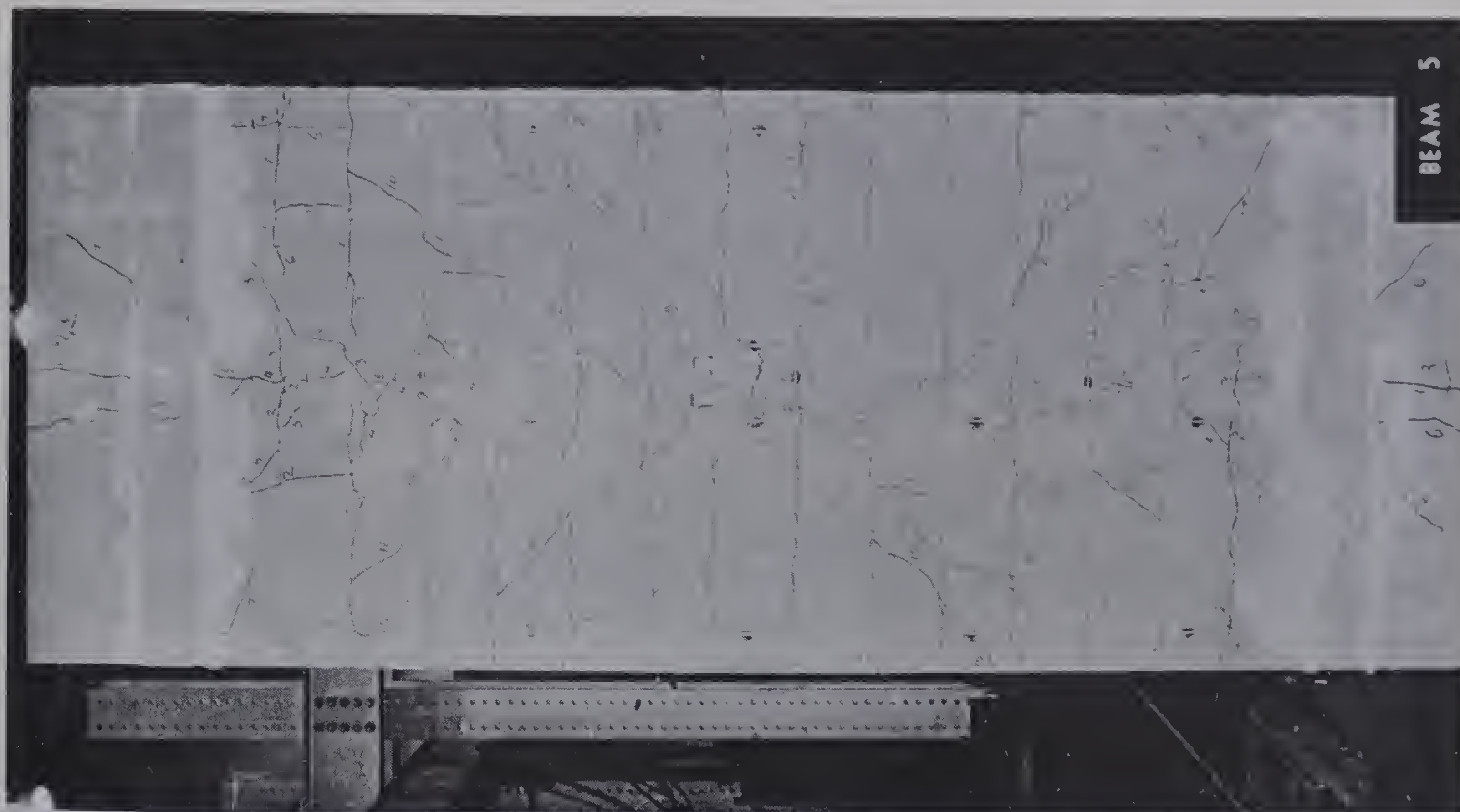

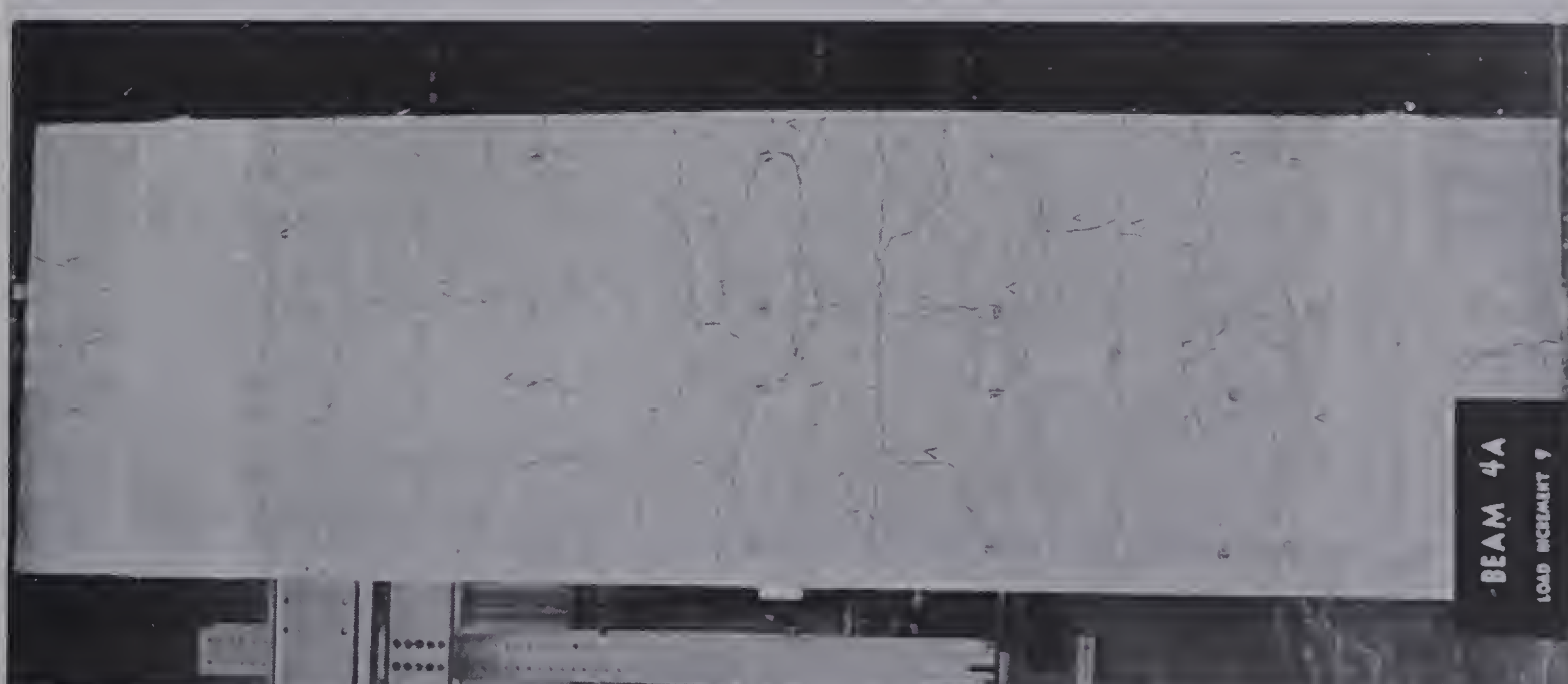

PLATE 4.5 CRACK PATTERNS

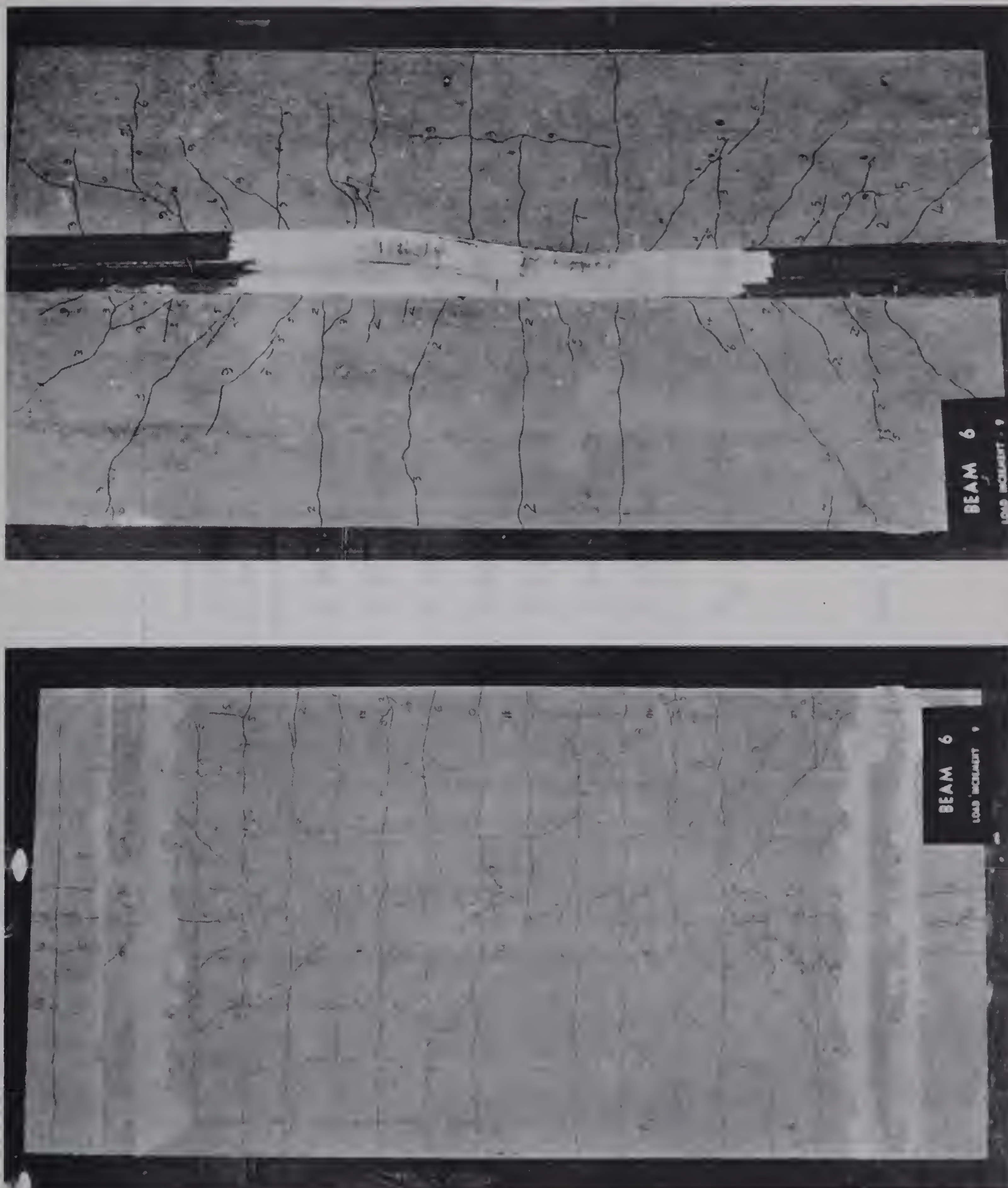

PLATE 4.6 CRACK PATTERNS

BEAM	COMPOSITE SECTION			STEEL SECTION			SLAB REINFORCEMENT	
	M_F (ft kips)	M_p (ft kips)	M_F/M_p	AREA (sq. in)	M_p (ft kips)	M_F/M_p	AREA (sq in)	% of BEAM AREA
1	188.3	179.9	1.047	5.94	98.4	1.91	3.10	52.2
2	178.0	169.9	1.048	5.94	98.4	1.81	2.48	41.7
3	114.0	116.7	0.978	4.86	76.1	1.50	1.86	38.4
4	110.0	103.2	1.066	4.86	76.1	1.42	1.20	24.7
4A	160.0	149.3	1.072	6.19	104.7	1.53	1.20	19.4
5	176.0	169.9	1.036	5.94	98.4	1.79	2.48	41.7
6	180.0	169.9	1.060	5.94	98.4	1.83	2.48	41.7

M_F - Moment at Failure M_p - Calculated Plastic Moment

TABLE 4.1 ANALYSIS OF ULTIMATE MOMENTS

BEAM	LONGITUDINAL REINFORCEMENT		NO. OF TRANSVERSE CRACKS IN 8 FT LENGTH	M/M_p AT START OF GENERAL CRACKING		
	AREA (sq. inch)	% OF SLAB AREA		DIAGONAL AT END	DIAGONAL AT MIDSPAN	LONGITUDINAL AT END
1	3.10	2.87	15	0.50	0.83	0.17
2	2.48	2.30	16	0.47	0.71	0.24
3	1.86	1.72	14	0.72	0.84	0.84
4	1.20	1.11	13	0.41	0.81	0.41
5	2.48	1.72	14	0.53	0.82	0.18
6	2.48	1.38	14	0.53	0.94	0.18

TABLE 4.2 SUMMARY OF CRACK DATA

CHAPTER V

DISCUSSION OF TEST RESULTS

5.1 GENERAL BEHAVIOUR

The beam tests are discussed below in the order in which tests were conducted.

BEAM 3 (3'-0" slab width, 6-#5 longitudinal bars)

BEAM 3 attained an ultimate load of 57 kips and failure occurred with little warning. The LOAD - DEFLECTION curve (FIGURE 4.1) deviated very little from a straight line up to the failure load. Failure was initiated by a local buckle of the compression flange and the web close to the loading jack. It was not possible to determine either by visual examination or by strain gauge readings whether the buckle started in the flange or the web.

This beam was designed with the highest load per shear connector. The slab was removed after the test in order to examine the connectors, but no deformation could be detected. PLATE 4.1 indicates the condition of these connectors.

BEAM 4 (3'-0" slab width, 6-#4 longitudinal bars)

BEAM 4 attained an ultimate load of 55 kips. The load-deflection curve exhibited only slightly more curvature before

failure than for BEAM 3. BEAM 4 also failed by local buckling as indicated in PLATE 4.2(a). Visual observation suggested that the failure started in the web, but this could not be confirmed by strain measurements. As soon as the specimen would no longer maintain load, it was unloaded. Little permanent deformation remained.

From the results of these first two tests, it was obvious that the remaining four beams would fail prematurely by local buckling. It was therefore decided to coverplate the remaining beams.

<u>BEAM 2</u> (3'-0" slab width, 8-#5 longitudinal bars)

The coverplate on BEAM 2 was welded with continuous welds except for about two inches of its length. This gap in the weld coincided with the gaugeline located 4 inches from midspan. Failure occurred very suddenly at 89 kips when the flange and coverplate separated and buckled at this unwelded portion as shown in PLATE 4.2(b).

<u>BEAM 5</u> (4'-0" slab width, 8-#5 longitudinal bars)

BEAM 5 held a load of 88 kips for several minutes and then began to deflect faster than the load maintainer could compensate. The load was reduced to 30 kips and the beam was then reloaded to 85 kips, at which load a lateral S-shaped buckle formed. This failure mode is shown in PLATE 4.3.

<u>BEAM 6</u> (5'-0" slab width, 8-#5 longitudinal bars)

BEAM 6 failed in a lateral buckling mode similar to that of BEAM 5 after maintaining a load of 90 kips for about five minutes.

<u>BEAM 1</u> (3'-0" slab width, 10-#5 longitudinal bars)

BEAM 1 failed in the lateral buckling mode upon reaching a load of 94.15 kips. The load deflection curve was still rising quite steeply just prior to failure.

<u>BEAM 4A</u> (3'-0" slab width, 6-#4 longitudinal bars)

Because BEAM 4 had suffered little visible damage other than cracking of the slab, it was subsequently coverplated and retested as BEAM 4A. It failed at a load of 80 kips in a lateral buckling mode.

5.2 CRACKING BEHAVIOUR

PLATES 4.4, 4.5, and 4.6 illustrate the cracking behaviour of the test specimens. Cracks are marked with load increment numbers. The cracks marked "0" are due to shrinkage prior to the test. The cracks marked "A" on BEAM 4 occurred when the beam was retested as BEAM 4A. For this second test, cracks were only marked at the completion of the test. Numerical data derived from the crack patterns is presented in TABLE 4.2.

The flexural cracking behaviour varied very little from beam to beam. Transverse flexural cracks formed in the concrete slabs at relatively low loads, usually during the first load increment. This cracking continued until transverse cracks had formed about six inches apart for beams with higher steel percentages and about seven inches apart for beams with lower steel percentages. Cracking did not start at midspan and progress towards the ends of the beam, but occurred over the entire length of the beam from the outset. Cracks were only slightly closer spaced at midspan than near the supports. The pattern of transverse cracks was no doubt influenced by shrinkage forces in the concrete. However, the nearly equal spacing of cracks indicates that partial loss of interaction between the steel beam section and slab reinforcement occurred even at low loads.

The second stage in the development of the crack pattern was the formation of diagonal cracks which formed at about 45 degrees to the flexural cracks. They usually occurred first near the ends of the beam at a load approximately half the ultimate load. As loading continued, the diagonal cracking progressed towards midspan and became general at midspan at a load approximately 80% of the ultimate load. The variation for individual beams from this general behaviour is noted in TABLE 4.2.

Accompanying the diagonal cracking was the development of short cracks oriented at angles between that of the diagonal and transverse cracks. Diagonal cracking is due to shear transfer and the cause of these shorter cracks is probably a combination of

shear and flexure. The formation of these short cracks, and to a lesser extent the diagonal cracks, was greatly influenced by the percentage of longitudinal reinforcement in the slab. BEAMS 3 and 5, which had different slab width and amounts of reinforcement, but the same steel percentage, exhibited very similar crack patterns. BEAMS 1 and 2 with the greatest steel percentages had the greatest number of cracks. BEAM 4, with the lowest steel percentage, had the least number of cracks. As the number of cracks increased, the average crack width decreased.

Also common to all beams was the formation of longitudinal cracks at the ends of the slab roughly along the line of the shear connectors. These cracks formed quite early in the loading except for BEAMS 3 and 4. The explanations for these cracks may be that the portion of slab between the end of the slab and the crack closest to the end acts as a cantilever beam supported at the center by the shear connectors, and loaded with the tension forces in the longitudinal slab reinforcement. If this is so, the cracks would be caused by flexural tension stresses.

Another type of longitudinal crack was peculiar to BEAMS 4 and 6. These two beams had the lowest amount of slab reinforcement per cross sectional area of concrete slab. The first time BEAM 4 was tested, only slight diagonal cracking occurred in the concrete slab. When the slab was examined after the second test (Beam 4A) very little additional diagonal cracking was observed, but considerable longitudinal cracking was in

evidence. The final load increments produced longitudinal cracking in BEAM 6 also. The formation of these longitudinal cracks explains the difference in magnitude of deflections observed between BEAMS 4A and 6, and the others tested (FIGURE 4.4)

Most cracks did not extend through the depth of the slab. The relative amount of cracking on the top and underside of BEAM 6 is shown in PLATE 4.6. BEAM 6 is typical except that only in BEAM 6 did longitudinal cracking appear on the underside of the slab. At final failure two or three cracks opened very wide, while the remainder seemed to be affected very little.

5.3 FAILURE MODES AND ROTATION CAPACITY

5.3.1 GENERAL

As previously noted, all test specimens failed when local or S-shaped lateral buckles formed in the compression flange of the steel beam. The failure by local buckling occurred when the compression flange of the 12B16.5 was not reinforced, as in BEAMS 3 and 4. Failure by lateral buckling occurred when the compression flange of the 12B16.5 was reinforced by a coverplate such as for BEAMS 1, 4A, 5 and 6. BEAM 2 was a special case for which a local buckle formed even though the compression flange was reinforced by a coverplate along the entire length except for a 2-inch gap in the welding.

The testing equipment used was designed to maintain load, not deflection. No workable method was found to stabilize

the system after the ultimate load had been reached. As a result measurements of midspan curvature and end rotation at failure or subsequent to failure were not taken. However, some qualitative data for deflections at and subsequent to failure was obtained. From this data and the well documented behaviour prior to failure, the effect of the failure modes on the rotation capacity can be discussed.

5.3.2 LOCAL BUCKLING

Prior to failure, the load deflection curves for BEAMS 3 and 4 were nearly linear, particularly for BEAM 3. When failure did occur, deflections increased rapidly. The LOAD - DEFLECTION curve for BEAM 2 flattened appreciably prior to failure similar to the behaviour of the beams which failed by lateral buckling. However, when failure did occur, it was sudden, almost violent. The sudden decrease in moment capacity associated with the formation of the local buckling is undesirable and indicates that BEAMS 2,3, and 4 had a very limited rotation capacity.

The 12B16.5 section is classified as a compact section by CSA Specification S16. Haaijer and Thurlimann[11] recommend width-thickness ratio limits for compact sections based on theoretical analysis and experimental investigation. From their analysis and tests, a section meeting the suggested width-thickness ratio restrictions can be strained into the strain-hardening range, and subsequent buckling should not be accompanied

by a drop in moment capacity. However, strain readings on the 12B16.5 used in beams of this investigation indicated that little strain hardening had occurred in BEAMS 3 and 4 before local buckling occurred. The buckling of the beams used in this investigation before expected on the basis of the work of Haaijer and Thurlimann may be due to the method of applying load. The fact that at high loads the strains measured by the electrical resistance strain gauges were significantly higher than the average strains measured by the Demec gauge indicates that the method of applying load did have an effect. But it may also be that the buckling behaviour of a structural steel section in a composite beam is sufficiently different from the buckling behaviour of that steel section used alone that the provisions for structural steel design cannot be applied to the design of composite sections.

Local buckling of the flanges at a width-thickness ratio of about 15 agrees with the findings of Daniels and Fisher[6,7].

5.3.3 LATERAL BUCKLING

Only beams with a coverplate on the compression flange failed by lateral buckling. For beams developing a lateral buckle, deflections increased slower after ultimate load had been reached than for BEAMS 2, 3, and 4. This indicated that the beams failing by lateral buckling had a much better rotation capacity than those failing by local buckling. The stiffeners on the steel section seemed to provide very effective lateral support to the

compression flange. It was noticed on one beam that the flange above the stiffeners yielded rather than participate in the lateral buckle. This indicates that the rotation capacity might be improved by providing stiffeners at more frequent intervals. The failure of beams by lateral buckling with a width-thickness ratio for the flange of about 6 agrees with the findings of Barnard[5].

5.4 MOMENT CAPACITY

The plastic moment capacity, as previously defined, was used in this investigation in order to study the effects on the moment capacity of variation of longitudinal reinforcement and the presence or absence of a coverplate. The plastic moment capacities, and the comparison of actual to computed moments are presented in TABLE 4.1. The computed moment capacities are based on average measured steel properties for BEAMS 1 to 6, and on average properties modified to account for strain hardening of the compression flange for BEAM 4A.

The test beams can be considered in two groups; beams with constant flange width and variable slab reinforcement, and beams with variable flange width and constant reinforcement. This second group of beams (BEAMS 2, 5, and 6) exhibited no significant variation in moment capacity. The 2 kip range of failure loads is well within experimental variation expected.

Flange width, therefore, had no appreciable effect on moment capacity over the range of variation considered in this investigation.

BEAM 3, the only beam failing at less than the predicted moment, failed at 97.8% of the calculated plastic moment. This fact, combined with the particularly poor rotation capacity and deflection behaviour exhibited by this beam, suggest that the failure of BEAM 3 was a premature failure. The remaining 6 tests yielded failure moments 3.6% to 7.2% above the calculated plastic moment. This indicates either that both the coverplate and slab reinforcement were adequately accounted for in the plastic moment computations, or that these two effects tend to balance each other. Because the strain measurements taken from the longitudinal reinforcement indicates that most of the reinforcement did not yield, it is likely that the behaviour assumed by the plastic moment computations does not occur.

Close agreement between experimental and predicted behaviour may have occurred because the contribution of the slab reinforcement to the moment capacity was smaller than predicted, but the contribution of the steel section was greater than predicted. Tests to determine the moment capacity of structural steel sections as reported by the Joint WRC-ASCE Committee on Plasticity[12] indicate that the actual ultimate moment for wide flange shapes may be greater than the calculated plastic moment by more than 20%. Ferrier[1] concluded from his investigations that an

increase in moment capacity occurred due to strain hardening in the steel beam section during positive bending of composite beams. In order to bring the predicted moment capacity of composite beams in negative bending to the same theoretical basis as for composite beams in positive bending and for structural steel members, it may be necessary to reduce the assumed stress in the slab reinforcement below the yield stress value assumed in computations for the tables and charts of this investigation. However, at least for the beams of this series, the plastic moment capacity did provide a simple and fairly accurate estimate of the failure moment providing premature failures were prevented.

A design criterion for prevention of premature buckling failures cannot be established on the basis of these tests. However, since the computed plastic moment was achieved by BEAM 4 it appears that a composite section consisting of a compact steel section and a concrete slab containing a longitudinal reinforcement area less than about 25% of the area of the steel section should develop the computed plastic moment. However, the rotation capacity of such a section may be quite small. Further research is required to determine for composite beams the width-thickness ratios which will ensure sufficient rotation capacity.

Tabulated in FIGURE 4.1 are values of the area of slab reinforcement as a fraction of the area of the steel section for

the beams tested. Also tabulated is the experimental ultimate moment attained by each beam as a fraction of the plastic moment capacity computed for the steel section used alone. It can be seen that for BEAM 4 an increase in total steel area (over that for the 12B16.5 section alone) of 25% increased the moment capacity by 42%. For BEAM 1 an increase in total steel area of 52% increased the moment capacity by 91%. Even though this comparison does not consider the actual ultimate capacities of the steel sections acting alone, it can be seen that significant increases in moment capacity can be achieved economically.

5.5 SLAB REINFORCEMENT STRAINS

5.5.1 GENERAL

LONGITUDINAL STRAIN PROFILES for the slab reinforcement are presented in FIGURES 4.11 and 4.12 and TRANSVERSE REINFORCEMENT STRAINS are presented in FIGURE 4.13. The points plotted in FIGURE 4.11 represent, with few exceptions, the average readings of two symmetrically placed gauges. Even these averages are fairly erratic, due mainly to the effect on the reinforcement strains of the cracking of the slab, and out-of-plane bending of the beam.

5.5.2 EFFECT OF FLANGE WIDTH

FIGURE 4.12 illustrates the strains measured for the longitudinal reinforcement of BEAMS 5 and 6. The pattern of strains exhibited by these two beams differs from that exhibited

by BEAM 2 (FIGURE 4.11) indicating a different behaviour for the beams of the greater slab widths.

In the TRANSVERSE STRAIN PROFILES of FIGURE 4.12 it can be seen that for BEAMS 5 and 6 the strains in the slab reinforcement decrease as the distance from the steel section increases, at least for the later stages of loading.

The LONGITUDINAL STRAIN PROFILES for BEAMS 5 and 6 are difficult to evaluate because of the limited number of gauges used. It can be noted from the gauge readings as a whole that the yield strain (approximately 1500 micro inches/inch) was not reached in all of the bars.

5.5.3 EFFECT OF REINFORCEMENT AREA

From the LONGITUDINAL STRAIN PROFILE of FIGURE 4.11 it can be noted that in six instances, the strains of the middle bars departed from what would be considered the normal behaviour. At these six locations, the strains increased normally with increasing load for several load increments, then the strains started to decrease with further load and finally in four instances the strains reversed in direction. This behaviour is unexpected and difficult to explain, but sufficient evidence of these strain decreases and reversals was recorded to discount the possibility of the gauges being faulty. It can be noted that this peculiar behaviour does not occur for the Edge Bars of these beams.

No close correlation between the crack patterns and these strain reversals could be found, but in general, development of the strain reversals coincided with diagonal cracking in the beams near the gauges. It can also be noted that the development of the strain reversals became more pronounced as the amount of slab reinforcement was increased. A nearly uniform strain distribution across the slab width is indicated for BEAM 4, but for BEAMS 1 and 2 the strain distribution is very irregular.

Without strain measurements from all bars in the slab, a satisfactory explanation of this unusual behaviour is probably not possible, but occurence of the strain reversals with increasing slab reinforcement and approximately coincident with diagonal cracking indicates that it may be due to transfer of shears in the slab.

The strain measurements of FIGURE 4.11 indicate that for BEAMS 1 to 4 yielding of the slab reinforcement was not general.

5.5.4 TRANSVERSE REINFORCEMENT STRAINS

TRANSVERSE REINFORCEMENT STRAINS are illustrated in FIGURE 4.13. The gauges to measure these strains were placed along the longitudinal centerline of the beam close to midspan (FIGURE 3.3) on the assumption that these would be points of maximum stress. From the crack patterns it would appear that the maximum transverse stresses occurred at the ends of the beams.

FIGURE 4.13 does indicate that the strains in the transverse reinforcement increased either with increasing amounts of longitudinal reinforcement or with increasing beam curvatures. Either interpretation would seem to be justified.

5.6 DEFLECTION BEHAVIOUR

Four gauges were used to measure deflections at midspan of the test beams. Two gauges were placed on the tension flange of the steel section, and two were placed on the edges of the concrete slab. The average deflections of the steel section are presented in FIGURES 4.1, 4.2, and 4.3. FIGURE 4.4 gives the average readings of these two sets of gauges in the form COMPARISON OF EDGE AND CENTER LINE DEFLECTIONS. In FIGURE 4.4, a positive value indicates the edge of the slab deflected more than the tension flange of the steel beam section. A negative value indicates that the edges of the slab deflected less than the steel section.

When a non-dimensionalized vertical scale is used to plot the LOAD - DEFLECTION curves, the curves are very similar. The COMPARISON OF EDGE AND CENTER LINE DEFLECTIONS indicates that, in general, the edges of the slab deflected less than the center line. These differences in deflection are fairly small but increase with increasing slab width. Two exceptions to this general behaviour are BEAMS 1 and 4A. For these beams the edges of the slab deflected more than the center line.

In addition to the center line deflection measurements, some beams were instrumented to measure the separation between the edge of the slab and the transverse support beams. Measurements indicated that separations in the order of 0.01 inches did occur with the largest separations occurring with the widest slabs.

5.7 END ROTATIONS AND CURVATURE DISTRIBUTION

It can be noted from FIGURES 4.9 and 4.10 that when the Center Line Curvatures for the beams are compared on the basis of the computed plastic moment capacities of the beams, their behaviour is very similar. The same can be said for the deflection behaviour of the test beams (FIGURES 4.2 and 4.3). However, the End Rotation curves (FIGURES 4.6 and 4.7) show a difference in behaviour. Curves for BEAMS 1 to 4 are very similar, but the curves for BEAMS 4A, 5 and 6 are different from each other and from curves of the remaining beams. The only logical explanation for this similarity of Deflections and Center Line Curvatures, but difference of End Rotations is that the distributions of curvatures along the length of the test beams must differ. Only for BEAM 2 was any data obtained concerning the distribution of curvature along the beam.

The curvatures determined from Gauge Line #2 of BEAM 2 are plotted on FIGURE 4.15, as are the Center Line Curvatures for BEAM 2. Rather than increasing at an increasing rate with moment

as did the curvature at the center line, the curvatures at Gauge Line #2 increased at a slower rate at high loads and finally on the last load increment, the curvatures actually decreased.

This unusual behaviour may tentatively be explained as follows: The forces in the steel in a composite section are due either to the curvatures in the steel section or to the strains in the slab reinforcement. An increase in either the curvature of the steel section or the reinforcement strains will increase the moment. The strains in the reinforcement are influenced by cracking of the slab, slip and bond failures, as well as the bending of the composite beam. It is conceivable that for any particular increment of load, the strains in the reinforcement at a particular section may increase considerably. This may result in an increase of reinforcement force greater than that required to increase the internal moment to balance the increase in external moment. Then, in order to decrease the internal moment and maintain equilibrium, the curvatures in the steel section must decrease.

Very little can be determined from one additional set of gauges on one beam about the distribution of curvatures in composite beams generally. However, the behaviour recorded by this set of gauges may be significant in that there may be a tendency for the plastic hinge length for composite beams to be compressed from the length expected by experience with structural steel sections.

5.8 CALCULATED VALUES

A computer program designed to simulate composite beams was used to produce tables of combinations of moment, strain, and position of the neutral axis for the composite sections as functions of center line curvature and degrees of interaction between the steel section and the slab reinforcement. From these tables, the combinations of moment, curvature and neutral axis position most closely duplicating the experimental results for any load increment were chosen. FIGURES 4.14 to 4.17 illustrate the agreement between experimental and calculated MOMENT-CURVATURE RELATIONSHIP and FIGURES 4.18 and 4.19 illustrate the agreement in position of the neutral axis. Any variation between the experimental curves and the calculated values for any of the FIGURES 4.14 to 4.19 indicates an inconsistency between actual behaviour and the assumptions made. Agreement is reasonably good for all the beams and also for Gauge Line #2 of BEAM 2, even though the program does not consider tension in the concrete or residual stresses in the steel.

The calculated values are analysed two ways. FIGURES 4.20 and 4.21 present MOMENT - INTERACTION FACTOR VALUES for the test beams and FIGURES 4.22 and 4.23 present MOMENT - SLAB TENSION FORCE values.

The interaction factor curves differ somewhat from beam to beam, but the general trend is the same. If a mathematical

shape can be established for the Interaction Factor curve, it could be used in calculations to predict moment curvature relationships for composite beams. The slab tension force curves are more regular than the interaction factor curves and possibly they could be used more easily to predict composite beam behaviour. At present the shape of these curves at values of moment near ultimate is not too well defined because of lack of data.

The calculated slab tension forces were compared to the possible tension forces assuming fully yielded reinforcement to determine the average stress in the reinforcement. The values for individual beams ranged from 70% of the yield stress for BEAM 3 to 100% of the yield stress for BEAM 4A with an average for all seven beams of about 88%.

CHAPTER VI

SUMMARY, CONCLUSION AND RECOMMENDATION

6.1 SUMMARY

This investigation was intended to explore the behaviour of composite beams subjected to negative moment. To achieve this seven tests were made on simple span composite beams loaded to produce tension in the concrete. The main variables in this investigation were the width of the concrete slab and the amount of longitudinal reinforcement in the slab. In addition, the width/thickness ratios for the compression flange of the steel section were modified for some of the beams to change the mode of failure. Measurements of strains were taken for the slab reinforcement and for the steel beam section, as well as measurements of beam deflections and end rotations. The patterns of cracking in the slab were also recorded.

6.2 CONCLUSIONS

The most significant conclusions based on the results of this investigation are summarized as follows:

1. Significant increases in the moment capacity of composite beams in negative bending were achieved by the addition of longitudinal reinforcement to the slab.

2. The average stress in the longitudinal slab reinforcement at ultimate moment was less than the yield stress for the reinforcement.

3. The use of a steel beam section defined as a compact section under provisions of CSA Standard S16 did not guarantee adequate rotation capacity for the formation of a plastic hinge in a composite beam in negative bending.

4. Decreasing the width/thickness ratio of the compression flange improved the resistance of the steel section of the composite beam to buckling and increased the rotation capacity of the composite section.

5. Cracking behaviour of the concrete slab was affected by the percentage of longitudinal reinforcement in the slab.

6.3 RECOMMENDATION FOR DESIGN

Though much information is still needed concerning the behaviour of composite beams in negative bending before recommendations for code specifications can be made, it is tentatively recommended that in the computations for the plastic moment capacity, the stress in the slab reinforcement be limited to approximately 85% of the yield stress.

6.4 RECOMMENDATIONS FOR FURTHER RESEARCH

The following are suggested as topics for further experimental and analytical investigation:

1. Width/thickness ratios and their effect on the buckling behaviour of the web and compression flange of composite beams.

2. Rotation capacity of composite beams in negative bending.

BIBLIOGRAPHY

1. Ferrier, D., "Moment Curvature Relationship of Composite Steel and Concrete Beams", Masters Thesis (unpublished) Dept. of Civil Engineering, University of Alberta, November 1965.

2. Siess, C.P., and Viest, I.M., "Test of Continuous Right I-Beam Bridges", University of Illinois Engineering Experiment Station; Bulletin Series No. 416.

3. Culver, C., Zarzeczny, P.J., and Driscoll, G.C. Jr., "Test of Composite Beams for Buildings" Progress Report 2, Fritz Engineering Laboratory Report No. 279.6, January, 1961.

4. Slutter, R.G., and Driscoll, G.D. Jr., "Test Results and Design Recommendations Composite Beams for Buildings" Progress Report 3, Fritz Engineering Laboratory Report No. 279.10, January 1962.

5. Barnard, Peter R., "On the Collapse of Composite Beams" a dissertation submitted to the University of Cambridge for the degree of Doctor of Philosophy, Corpus Christi College, September 1963.

6. Daniels, J.H., and Fisher, J.W., "Fatigue Behaviour of Continuous Composite Beams", Fritz Engineering Laboratory Report No. 324.1, December 1967.

7. Daniels, J.H. and Fisher, J.W., "Static Behaviour of Continuous Composite Beams", Fritz Engineering Laboratory Report No. 324.2 March 1967.

8. Culver, C., Coston, R., "Tests of Composite Beams with Stud Shear Connectors", Proceedings of the American Society of Civil Engineers (Structural) Volume 87, Part 2, 1961.

9. Driscoll, G.C. Jr., Slutter, R.G., "Research on Composite Design at Lehigh University", Fritz Laboratory Reprint No. 180 - Reprinted from Proceedings of the American Institute of Steel Construction, 1961.

10. Bethlehem Steel Design File, "Properties of Composite Sections for Bridges and Buildings", AIA File No. 13.

11. Haaijer, G., and Thurlimann, B., "Inelastic Buckling In Steel" Paper No. 3023, Transactions, ASCE, Vol 125, 1960.

12. The Joint WRC-ASCE Committee on Plasticity Related to Design, "Commentary on Plastic Design in Steel: General Provision and Experimental Verification", Progress Report No. 2, Journal of the Engineering Mechanics Division, Proceedings of the ASCE, July 1959.